

Stein Boltzmann Sampling: A Variational Approach for Global Optimization

Gaëtan Serré Argyris Kalogeratos Nicolas Vayatis
École Normale Supérieure Paris-Saclay, Centre Borelli, France
name.surname@ens-paris-saclay.fr

Abstract

In this paper, we present a flow-based method for global optimization of continuous Sobolev functions, called *Stein Boltzmann Sampling* (SBS). SBS initializes uniformly a number of particles representing candidate solutions, then uses the *Stein Variational Gradient Descent* (SVGD) algorithm to sequentially and deterministically move those particles in order to approximate a target distribution whose mass is concentrated around promising areas of the domain of the optimized function. The target is chosen to be a properly parametrized Boltzmann distribution. For the purpose of global optimization, we adapt the generic SVGD theoretical framework allowing to address more general target distributions over a compact subset of \mathbb{R}^d , and we prove SBS's asymptotic convergence. In addition to the main SBS algorithm, we present two variants: the SBS-PF that includes a particle filtering strategy, and the SBS-HYBRID one that uses SBS or SBS-PF as a continuation after other particle- or distribution-based optimization methods. A detailed comparison with state-of-the-art methods on benchmark functions demonstrates that SBS and its variants are highly competitive, while the combination of the two variants provides the best trade-off between accuracy and computational cost.

1 Introduction

We consider the problem of global optimization of an unknown a priori nonconvex, continuous Sobolev function, under the concern of making efficient use of the computational budget. Optimizing an unknown function is a typical situation in real applications, as hyperparameter calibration or complex system design emerge in several domains (e.g. [19, 29]). For this purpose, sequential methods are usually employed, where at each iteration the algorithm uses information extracted from the previous candidate solutions to propose the new ones. Sequential and stochastic methods have been proposed to address this problem, and recent results [5, 14, 39] show that only stochastic algorithms can approximate optimal points of an arbitrary Lipschitz function. Sequential methods rely on a sampling process to explore the search space, and a selection process to choose the next candidate solutions using the information given by the previous ones.

In this work, we introduce a new sequential and deterministic flow-based method, called *Stein Boltzmann Sampling* (SBS), for continuous Sobolev functions. SBS uses the *Stein Variational Gradient Descent* (SVGD) [21] method to sample from a target distribution whose mass is concentrated at areas of the domain where minimizers are possible to be found. We choose as target the Boltzmann distribution (BD), which by definition converges toward a distribution supported on all minimizers of the optimized function. The idea of sampling from the BD to approximate minimizers of a function is not new (e.g. [2, 4]), yet utilizing SVGD for global optimization is novel, and therefore, part of our contribution concerns the adaptation of the generic SVGD theoretical framework for our objective. SVGD is a generic variational inference method that approximates a target distribution. More specifically, SVGD constructs a flow in the space of probability measures (similarly to a gradient

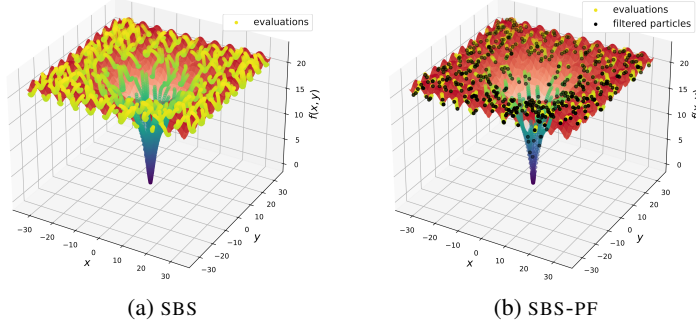


Figure 1. Illustration of the flow of measures and the trajectories of particles over the iterations. The color gradient represents the 2d Ackley function value, from blue (low) to red (high). The trajectories draw the discretized flow of measures. **a)** SBS: the particles are initialized uniformly at random over the domain, and then get updated by making a small step in the direction induced by SVGD forces. **b)** SBS-PF variant with particle filtering: the particles are initialized and updated as before, but the unpromising ones get rapidly removed and are not replaced. This is visible as there are less persisting trajectories in areas where the function has high values. This strategy results in a significant reduction of the budget while having comparable performance.

flow evolving in \mathbb{R}^d) that moves toward the target distribution. In the discrete case, candidate solutions are represented by particles, and their updates are affected by attraction and repulsion forces. The SBS optimization process is illustrated in Fig. 1 (some elements will be clarified in Sec. 3), where the sequence of updates over the candidate solutions are shown as trajectories of particles aiming to reach the global minimum.

The related global optimization literature is rich of methods. Namely, ADALIPO [25] is a method that is consistent over Lipschitz functions and is adapted for a very low computational budget (i.e. function evaluations at candidate minimizers). Also adapted for low budget, there is the well-known BAYESOPT method [26]. Then, there are existing approaches that use MALA to sample from the Boltzmann distribution, in a similar way to our method [8, 11, 30, 38]. CMA-ES [12] and WOA [28], are two inconsistent methods but known to be very efficient in practice. Due to either early stopping conditions or time complexity, these two methods do not scale well computationally, hence they are not suited for when the available budget is low. The recent method in [31] subsamples a finite subset of constraints from an uncountable one and uses an SDP solver to approximate the global minimum.

The rest of the contribution of the paper, is as follows: we provide a new proof of the asymptotic convergence of SVGD over a compact subset of \mathbb{R}^d for a class of target distributions. The class of distributions considered is more general than the one usually considered in the literature, and allows to show the convergence of SBS for any continuous Sobolev function. In the appendix, we provide detailed definitions and results of the SVGD theory, adapted in the context of global optimization. To ensure the correctness and reproducibility of the technical proofs, we provide for some of the results links to proofs in the Lean proof assistant [6, 27]. Then, we introduce two SBS variants: one that uses particle filtering to reduce the budget needed (see Fig. 1b), and a hybrid one that uses SBS as a continuation of CMA-ES or WOA, to combine their efficiency with the consistency and scalability of our method. Finally, we compare our approach with five state-of-the-art methods on several standard global optimization benchmarks. Finally, we interpret, in our context, the internal attraction and repulsion forces between particles, which come in effect during the SVGD sampling.

Notations. $d \in \mathbb{N}$ is the dimension of the optimization problem; $f : \Omega \rightarrow \mathbb{R}$ is the function to optimize, its domain $\Omega \subset \mathbb{R}^d$ is a smooth, connected and compact set; $x^* \in X^*$ is one of the global minima of f , i.e. $\forall x^*, f^* = f(x^*)$. Given an arbitrary function f , its support is $\text{supp}(f) = \{x \in \Omega \mid f(x) \neq 0\}$. Let λ be the standard Lebesgue measure on the Borel sets of \mathbb{R}^d . We denote by C^p the set of p -times continuously differentiable functions, and by $C_c^\infty(\Omega)$ the set of smooth functions on Ω that have compact support. Given two measurable spaces (Ω_1, Σ_1) and (Ω_2, Σ_2) , a measurable function $f : \Sigma_1 \rightarrow \Sigma_2$ and a measure μ over Σ_1 , let $f_\# \mu$ denote the pushforward measure, i.e.

$$\forall B \in \Sigma_2, f_\# \mu(B) = \mu(f^{-1}(B)).$$

For any $m, p \in \mathbb{N}$, let $W^{m,p}$ be the Sobolev space of functions with m weak derivatives in $L_\mu^p(\Omega)$:

$$W^{m,p} \triangleq \{f \in L_\mu^p(\Omega) \mid \forall \alpha \in \mathbb{N}^d, |\alpha| \leq m, D^\alpha f \in L_\mu^p(\Omega)\},$$

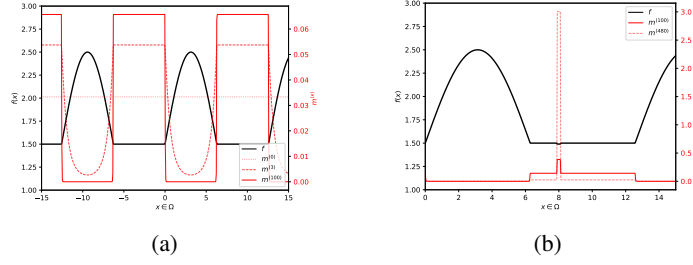


Figure 2. **a)** The density of the Boltzmann distribution $m^{(\kappa)}$ (Definition 2.1), shown in red lines, becomes uniform over the set of minimizers X^* of the given function f to optimize, as its parameter κ grows and tends to infinity. **b)** In this example, the volume of the set X^* is much smaller than the volume of local minimizers in the flat region. The value of the function at the local minimizers is close to the value of the global ones. A value of $\kappa = 100$ suffices to concentrate the majority of the mass of $m^{(\kappa)}$ around the global minimizers.

where D^α is the weak derivative operator w.r.t. to the multi-index α , and μ is clarified by the context. Let the Hilbert space H^m be the Sobolev space $W^{m,2}$.

The reader may find useful the full list of notations provided in the appendix (see Tab. 3).

2 Stein Boltzmann Sampling

2.1 The proposed method

Let us now introduce the *Stein Boltzmann Sampling* (SBS) method. The main idea proposed is to adapt the *Stein Variational Gradient Descent* (SVGD) sampler for the purpose of global optimization. While SVGD has been thoroughly studied in the literature [7, 17, 20, 23, 34], employing it in a global optimization context has not been previously considered. Part of the contribution of this work is, therefore, to adapt the SVGD theoretical framework so as to be suitable for global optimization, and to allow to address more general target distributions over Ω . For consistency and completeness, we prove classical results in the adapted framework in Appendix A.2.

Given an initial measure μ , SVGD constructs iteratively a sequence of measures that get closer to a target distribution π , in terms of KL-divergence. The update direction is given by:

$$\phi_\mu^* = \mathbb{E}_{x \sim \mu} [\nabla \log \pi(x) k(\cdot, x) + \nabla_x k(\cdot, x)], \quad (1)$$

where the gradient operator is understood in the sense of distributions, and k is the reproducing kernel of a specific RKHS \mathcal{H} (see Appendix A.2 for more details). Since the density of π appears in a gradient-log term, the normalization constant that classically emerges in Bayesian inference vanishes. In practice, the sequence of continuous measures constructed by SVGD is discretized to a sequence of particles, which are then updated using Eq. 1 (see Sec. 2.3).

To use SVGD as a global optimization method, we need a target distribution that concentrates its mass around the global minimizers of the optimized function. The continuous Boltzmann distribution (BD), has this feature. Moreover, it is a classical object in the global optimization theory, and it makes a link between our method and the simulated annealing method [16] (see Sec. 6).

Definition 2.1 (Continuous Boltzmann distribution). Given a function $f \in C^0(\Omega, \mathbb{R})$, the Boltzmann distribution over f is induced by the probability density function $m_{f,\Omega}^{(\kappa)} : \Omega \rightarrow \mathbb{R}_{\geq 0}$ defined by:

$$m_{f,\Omega}^{(\kappa)}(x) = m^{(\kappa)}(x) = \frac{e^{-\kappa f(x)}}{\int_{\Omega} e^{-\kappa f(t)} dt}, \quad \forall \kappa \in \mathbb{R}_{\geq 0}. \quad (2)$$

A characteristic property of the BD is that, as κ tends to infinity, the BD tends to a distribution supported only over the set of minimizers X^* . If $\lambda(X^*) > 0$, the BD tends to a uniform distribution over X^* (see Fig. 2a). If $\lambda(X^*) = 0$, it tends to a distribution over X^* where the concentration of the mass depends on the local geometry of the minimizing manifolds [13] (see details in Appendix A.1).

Our SBS method is the SVGD sampler applied to the BD. Note that any distribution whose density has the characteristic of being asymptotically supported only over X^* could be used as a target distribution in the following theoretical results. The pseudocode of the proposed SBS method can be

found in Alg. 1. Our main contributions reside on the proof of the asymptotic convergence of SBS, that relies on an adapted version of the SVGD theoretical framework, and on the introduction of two variants of SBS that are more efficient in terms of computational budget.

2.2 Asymptotic convergence of SBS

First, let $\mathcal{P}_n(\Omega)$ be the set of probability measures on Ω such that for each element $\mu \in \mathcal{P}_n(\Omega)$:

$$\mu \ll \lambda \wedge \mu(\cdot) \in W^{1,n}(\Omega) \wedge \text{supp}(\mu(\cdot)) = \Omega,$$

where $\mu(\cdot)$ is the density of μ w.r.t. λ . To prove the asymptotic convergence of SBS, we need to prove that the sequence of measures constructed by SVGD, noted as $(\mu_i)_{i \in \mathbb{N}}$ (see details in Appendix A.2), converges to the distribution induced by the BD, noted as π . To do so, we need to study the flow of measures induced by the update direction of SVGD. To use theoretical results of our adapted SVGD framework, we need to ensure μ and π belongs to $\mathcal{P}_2(\Omega)$. For the latter, we assume that f is in $C^0(\Omega) \cap W^{1,4}(\Omega)$ so that $m^{(\kappa)}$ is in $H^1(\Omega)$ (see proof in Appendix B.2). Theorem 2.2 and Theorem 2.3 are known results in the literature that we prove in our adapted SVGD framework. Then, we introduce two lemmas that are crucial to arrive to the proof of asymptotic convergence of SBS.

Theorem 2.2 (Time derivative of a measure flow [20]). *Let $\phi : \mathbb{R}_{\geq 0} \times \Omega \rightarrow \Omega$, $\phi(t, \cdot) = \phi_t(\cdot)$ be a vector field and $\mu \in \mathcal{P}_2(\Omega)$. Let $(T_t)_{0 \leq t} : \Omega \rightarrow \Omega$ be a locally Lipschitz family of diffeomorphisms, representing the trajectories associated with the vector field ϕ_t , and such that $T_0 = I_d$. Let $\mu_t = T_{t\#}\mu$. Then, μ_t is the unique solution of the following nonlinear transport equation:*

$$\begin{cases} \frac{\partial \mu_t}{\partial t} = -\nabla \cdot (\phi_t \mu_t), \forall t > 0 \\ \mu_0 = \mu \end{cases} \quad (3)$$

where $(\nabla \cdot)$ is the divergence operator, in the sense of distributions (see details in Appendix B.7). Moreover, the sequence $(\mu_i)_{i \in \mathbb{N}}$, constructed by SVGD, is a discretized solution of Eq. 3, considering the vector field $\phi_{\mu_t}^*$. One can consider the resulting flow of measures:

$$\begin{aligned} \Phi : \mathbb{R}_{\geq 0} \times \mathcal{P}_2(\Omega) &\rightarrow \mathcal{P}_2(\Omega), \\ (t, \mu) &\mapsto \Phi_t(\mu) = \mu_t. \end{aligned}$$

We give a different proof of this theorem in Appendix B.7, using optimal transport theory. That proof is more general in T , but less constructive. We also prove that the sequence $(\mu_i)_{i \in \mathbb{N}}$ is a discretized solution of Eq. 3 (note that Eq. 3 has also been extensively studied in [23]). This result allows to study the time-derivative of the KL-divergence between μ_t and π . Let S_μ be an integral operator associated to \mathcal{H} , and $\mathfrak{K}(\mu|\pi)$ a discrepancy measure between μ and π in $\mathcal{P}_2(\Omega)$ called *Kernelized Stein Discrepancy* (KSD). Both objects are detailed in Appendix A.2. We have the following result.

Theorem 2.3 (Time-derivative of the KL-divergence [20]). *Let $(T_t)_{0 \leq t} : \Omega \rightarrow \Omega$ be a locally Lipschitz family of diffeomorphisms, representing the trajectories associated with the vector field $\phi_{\mu_t}^* = S_{\mu_t} \nabla \log \frac{\pi}{\mu_t}$, such that $T_0 = I_d$. Let $\mu_t = T_{t\#}\mu$. Then, the time derivative of the KL-divergence between μ_t and π is given by*

$$\frac{\partial \text{KL}(\mu_t|\pi)}{\partial t} = -\mathfrak{K}(\mu_t|\pi).$$

Moreover, as $\mathfrak{K}(\mu_t|\pi)$ is nonnegative, the KL-divergence is non-increasing along the flow of measures.

The proof is in Appendix B.8. In order to show the convergence of continuous-time SVGD, we proved that the KSD is a valid discrepancy measure.

Lemma 2.4 (KSD valid discrepancy). *Let $\mu, \pi \in \mathcal{P}_2(\Omega)$. Then,*

$$\mu = \pi \iff \mathfrak{K}(\mu|\pi) = 0.$$

The proof is in Appendix B.9. The previous lemmas imply directly that π is the unique fixed point of the flow of measures Φ .

Lemma 2.5 (Unique fixed point). *Let $\pi \in \mathcal{P}_2(\Omega)$ and Φ be the flow of measures defined in Theorem 2.2. Then, for any $t \geq 0$, π is the unique fixed point of $(\mu : \mathcal{P}_2(\Omega)) \mapsto \Phi_t(\mu)$.*

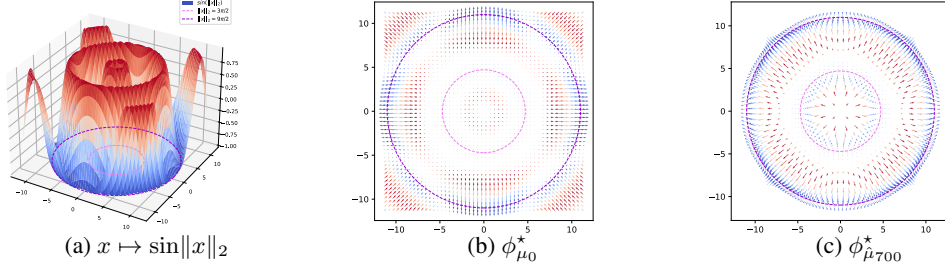


Figure 3. Illustration of the vector field ϕ^* in the discrete setting where π is the BD. **a)** The optimized function $x \mapsto \sin\|x\|_2$ and the two ring-shaped manifolds at which it is minimized (dashed lines). **b)** The initial particles (not shown) start getting attracted toward the two ring-shaped manifolds. **c)** After some SVGD iterations, there are stronger forces in the vector field and the particles get concentrated around those minimizing regions.

Since $\mathfrak{K}(\mu|\pi) = \|\phi_\mu^*\|_{\mathcal{H}}^2$ (see Appendix A.2), the proof is straightforward using the previous lemmas. The complete proof is in Appendix B.10. Finally, we prove next the weak convergence of μ_t to π .

Theorem 2.6 (Weak convergence of SVGD). *Let $\mu, \pi \in \mathcal{P}_2(\Omega)$. Let $(T_t)_{0 \leq t} : \Omega \rightarrow \Omega$ be a locally Lipschitz family of diffeomorphisms, representing the trajectories associated with the vector field $\phi_{\mu_t}^* = S_{\mu_t} \nabla \log \frac{\pi}{\mu_t}$, such that $T_0 = I_d$. Let $\mu_t = T_{t\#} \mu$. Then, we have that*

$$\mu_t \rightharpoonup \pi.$$

The proof is in Appendix B.11 and relies on Theorem 2.3 and Lemma 2.5; it is inspired by the proof of Theorem 2.8 in [23].

2.3 Discrete setting

In practice, SVGD is a discrete-time algorithm that iteratively updates a set of particles and not a continuous measure μ . It starts by sampling a sequence of particles from a distribution μ : $X = (x^{(1)}, \dots, x^{(N)}) \sim \mu^{\otimes N}$, and then each time it computes the next ones as follows:

$$X_{i+1} = X_i + \varepsilon \phi_{\hat{\mu}_i}^*(X_i), \quad \text{where} \quad \hat{\mu}_i(A) = \frac{1}{N} \sum_{j=1}^N \delta_{X_i^{(j)}}(A). \quad (4)$$

Fig. 3 provides an example illustrating two states of the vector field ϕ_t^* : the initial one at $t = 0$ and the one after 700 iterations, in the discrete setting where π is the BD. The previous results are sufficient to show the main theoretical result concerning SBS: its asymptotic convergence in discrete setting.

Theorem 2.7 (SBS asymptotic convergence). *Let $f : \Omega \rightarrow \mathbb{R}$ be in $C^0(\Omega) \cap W^{1,4}(\Omega)$. Let $\kappa > 0$ and let π be the BD (Definition 2.1) associated with f and κ . Let $\mu_0 \in \mathcal{P}_2(\Omega)$ and let $\hat{\mu}_i$ be defined by Eq. 4. Then,*

$$\left\{ f(X_i) \mid X_i = (x^{(1)}, \dots, x^{(N)}) \sim \hat{\mu}_i^{\otimes N} \right\} \xrightarrow[\substack{N \rightarrow \infty \\ \varepsilon \rightarrow 0 \\ i \rightarrow \infty \\ \kappa \rightarrow \infty}]{\quad} \{f^*\}.$$

The proof relies on three main elements: the almost sure convergence of the empirical measure $\hat{\mu}_i$ to μ_i , the weak convergence of μ_i to π using Theorem 2.2 and Theorem 2.6 (that are applicable as $f \in C^0(\Omega) \cap W^{1,4}(\Omega)$), and finally the fact that the BD tends to a distribution supported over the set of minimizers X^* as κ tends to infinity. The proof is provided in Appendix B.12.

To summarize, we proved that SBS is asymptotically convergent for any continuous function belonging to $W^{1,4}(\Omega)$. Note that, since Ω is compact, $C^\infty(\Omega) \subset W^{1,4}(\Omega)$, and therefore, the result holds for any smooth function on Ω . We adapted the SVGD theoretical framework for target distributions that are in $\mathcal{P}_2(\Omega)$ over a compact subset of \mathbb{R}^d (see Appendix A.2). This is a different to what is usually considered in the literature, where the target distribution density is smooth and its domain is the \mathbb{R}^d (e.g. [21, 22]). Some works have tried to relax the assumptions on the target distribution (e.g. [17, 34]). However, thanks to the compactness of Ω , our assumptions on π are less restrictive and only consider integration constraints on its 1st order weak derivatives, which makes our framework more adapted for global optimization.

The implementation of SBS uses Eq. 4 and estimates the gradients using finite differences. At each iteration, it updates the set of particles by a small step size in the direction induced by $\phi_{\mu_i}^*$, which is computed using the Adam optimizer [15]. We choose the initial distribution μ_0 to be the uniform distribution on Ω , as it maximizes the entropy (i.e. high initial exploration), and we also use the RBF kernel function. These two objects meet the requirements of the theory, and are used in most of the SVGD literature. To better understand the previous results and involved objects, we introduce a non-exhaustive list of definitions and theoretical results related to SVGD in Appendix A.2.

3 SBS variants

In addition to the main SBS method, we introduce two variants that can be more efficient in practice. The first one, called SBS-PF, uses a particle filtering approach that removes the less promising particles (without replacing them). The second one, called SBS-HYBRID, is a hybrid method that uses SBS as a continuation for other global optimization methods, or –seen the other way around– those methods are used to initialize SBS. SBS-PF uses less budget than SBS, and SBS-HYBRID uses some of the budget to run one of the pre-existing methods to initialize SBS with better starting points; the aim is to approximate the global minimum better than SBS with the same budget.

SBS-PF. We use a simple particle filtering idea: to remove particles (i.e. candidate minimizers of f) that are less promising or stuck in bad local minima. We chose to remove particles that do not move and correspond to significantly higher function values than the others. Therefore, this strategy is very likely to remove particles that are stuck in bad local minima. The difference between SBS and this variant is visualized in Fig. 1. One can see that, in SBS-PF, the unpromising candidates are rapidly removed and are not replaced so that the remaining particles are more likely to converge to the global minimum. This strategy results in a significant reduction of the budget used, while having comparable optimization results to SBS. Note that the strategy to prove Theorem 2.6 is not directly applicable to SBS-PF, thus, the asymptotic convergence of SBS-PF is not guaranteed. However, the empirical results show that SBS-PF is efficient in practice, and it is a good alternative to SBS when the budget is limited.

SBS-HYBRID. This variant is based on the idea of using SBS or SBS-PF as a continuation for particles- or distribution-based methods, such as WOA or CMA-ES. Indeed, the design of SBS allows to initialize the particles with the result of one such method, and then resume the optimization process with an SBS variant. More specifically, we introduce SBS-HYBRID that runs few iterations of both CMA-ES and WOA to choose the most promising result, and then continues the optimization with SBS (see Alg. 2). Both WOA and CMA-ES are efficient methods, thus, a small number of iterations allows to



(a) Log-distance between the computed solution and the global minimum vs. the value of κ for SBS.



(b) Execution time vs. the number of evaluations for BAYESOPT, ADALIPO and CMA-ES

Figure 4. Insights for the compared algorithms: **a)** shows the low impact of κ on the performance of SBS. **b)** shows the time to run for BAYESOPT and ADALIPO grows exponentially and is significantly higher than for CMA-ES. In each case (a) and (b), the **left** plot is for the Himmelblau, and the **right** is for the Levy function.

find a good starting point for SBS. Moreover, both methods are not well-suited for a large budget, but for different reasons: CMA-ES uses early stopping rules (i.e. for the covariance matrix to not become ill-conditioned), and WOA takes more time to run than SBS for the same budget. SBS-HYBRID can be seen as a combination of the asymptotically consistent SBS method, on top of very efficient but non-consistent methods. Among the strengths of SBS-HYBRID, we can mention that: i) it empirically provides high-quality results, and ii) it is still asymptotically consistent, since the initial distribution of the particles induced by WOA and CMA-ES meet the assumptions of Theorem 2.6.

4 Choice of hyperparameters

In this section, we discuss the choice of the hyperparameters of SBS and its variants. We focus on the choice of κ and σ , as they carry complex information about the behavior of the method. **Choice of κ .** As detailed earlier, κ controls the shape of the BD from which SVGD samples. The bigger κ is, the more the mass of the distribution gets concentrated around the global minima of the function. Intuitively, the optimal κ such that a satisfying amount of the mass to be around the global minima depends on the geometry of the function around local minima (the asymptotic behavior of the BD depends on the local geometry, see [13]). Nevertheless, one can see in Fig. 4a that, in practice, the choice of κ does not significantly affect the performance of SBS. The reason is that, if the modes of the BD that contain the most of the density mass are the ones around the global minima, then SVGD would succeed in moving some particles in the areas of those modes, provided there are enough particles. The three following parameters control how the mass is repartitioned: the value of κ , the ratio between the volume of the region of local minimizers and the volume of the region of global minimizers, and the value of the function at the local minimizers. These three parameters are interdependent: the value of one can compensate for the value of the others; one can create a function that requires a high κ for the majority of the mass to not be around the global minima (see Fig. 2). Thus, choosing a very large κ , such as 10^3 , will compensate potential issues related to the geometry of the function and ensure a good performance on average.

Choice of σ . All SBS variants use the RBF kernel with a bandwidth σ , the choice of which is crucial for their performance. As detailed in Sec. 6, the size of σ controls the forces that are developed between particles. When a lot of particles are close together, they repel each other. This behavior enforces the exploration of the function domain. However, it also prevents SBS from converging in narrow regions, where global minima could be located. A natural choice is $\sigma = \frac{1}{N^2}$, where N is the number of particles. This choice ensures that, when the particles are few, σ gets large enough and SBS explores the domain. On the other hand, with a lot of particles the exploration is ensured by the uniform initial distribution μ_0 and by the small induced σ that allows the particles to converge to the global minimum, even in narrow regions. For the SBS-PF variant, σ changes during the optimization process, as particles are being filtered out. For the SBS-HYBRID variant, as the initial particles are supposed to be close to the global minimum, σ is set to a very small value, e.g. $\sigma = 10^{-10}$.

Algorithm 1 Stein Boltzmann Sampling (SBS)

Input: $f : \Omega \rightarrow \mathbb{R}$; number of vectors (particles) N ; Boltzmann parameter κ ; step-size ε ; number of SVGD iterations n ; an initial distribution μ_0 over the particles
Output: \hat{x} , an estimate of x^*

Sample N particles: $X_1 \leftarrow (x^{(1)}, \dots, x^{(N)}) \sim \mu_0^{\otimes N}$
for $i = 1$ **to** n **do**
 Compute the vector field $\phi_{\mu_i}^*$ - - see Sec. 2.1
 $X_{i+1} \leftarrow X_i + \varepsilon \phi_{\mu_i}^*(X_i)$ - - update the particles
 $\hat{\mu}_{i+1} \leftarrow \frac{1}{N} \sum_{j=1}^N \delta_{X_{i+1}^{(j)}}$ - - empirical measure
end for
 $\hat{x} \leftarrow \arg \min_{1 \leq j \leq N} f(X_{n+1}^{(j)})$ - - the "best" particle
return \hat{x}

Algorithm 2 Initialization choice of SBS-HYBRID

Input: number of candidates N ; CMA-ES budget b
Output: N candidates

Run CMA-ES for b function evaluations
Run WOA with N candidates
if CMA-ES found a better value than WOA **then**
 Sample N candidates from the last Gaussian
else
 Use the N candidates from WOA
end if
return the N candidates

Table 1. Comparative results. Comparison between all SBS variants with several state-of-the-art methods on two dimensional benchmark functions. For each function, we report the average best function value found (lower is better). SBS-HYBRID runs 1K iterations of CMA-ES and WOA. As one can see, SBS-HYBRID and SBS respectively rank 1st and 3rd while SBS-PF-HYBRID and SBS-PF achieve competitive results with significantly less evaluations (respectively $\sim 67\%$ and $\sim 97\%$ budget reduction).

FUNCTIONS	STATE-OF-THE-ART					PROPOSED METHOD AND VARIANTS				
	LANGEVIN	BAYESOPT	ADALIPO	CMA-ES	WOA	SBS-PF	SBS	SBS-PF-HYBRID	SBS-HYBRID	
ACKLEY	12.779	0.322	1.286	9.916	9×10^{-8}	0.002	8×10^{-4}	1×10^{-5}	5×10^{-6}	
BRANIN	0.398	0.398	0.400	0.398	0.398	0.398	0.398	0.398	0.398	
DROP WAVE	-0.052	-0.838	-0.955	-0.685	-1.000	-0.963	-0.981	-0.934	-0.981	
EGG HOLDER	1049.132	-860.935	-937.983	-629.634	-959.641	-932.393	-958.142	-944.700	-946.280	
GOLDSTEIN PRICE	2548.300	10.231	3.813	37.236	3.000	3.000	3.000	3.000	3.000	
HIMMELBLAU	3×10^{-6}	6×10^{-4}	0.006	1×10^{-16}	3×10^{-6}	1×10^{-7}	9×10^{-11}	7×10^{-19}	9×10^{-21}	
HOLDER TABLE	-9.234	-19.169	-19.184	-10.843	-19.208	-19.209	-19.209	-19.209	-19.209	
MICHALEWICZ	-5×10^{-15}	-1.801	-1.790	-1.696	-1.801	-1.801	-1.801	-1.801	-1.743	
RASTRIGIN	4.944	2.780	0.191	4.155	4×10^{-15}	0.100	1×10^{-9}	0.497	0.398	
ROSENBROCK	0.534	0.106	0.037	1×10^{-15}	2×10^{-7}	4×10^{-5}	2×10^{-6}	5×10^{-17}	2×10^{-17}	
CAMEL	161.823	-0.967	-1.016	-1.032	-1.032	-1.032	-1.032	-1.032	-1.032	
LEVY	75.563	0.056	0.024	3.445	1×10^{-8}	9×10^{-8}	2×10^{-12}	1×10^{-19}	6×10^{-20}	
SPHERE	1×10^{-5}	8×10^{-4}	6×10^{-4}	2×10^{-16}	3×10^{-16}	8×10^{-8}	8×10^{-12}	2×10^{-19}	1×10^{-21}	
COMP. RATIO (CR)	85.732	92.385	92.385	54.309	31.511	69.558	33.567	31.462	28.331	
AVERAGE RANK	8.46	7.23	6.54	6.00	3.54	4.92	3.38	2.77	2.15	
FINAL RANK	9	8	7	6	4	5	3	2	1	

5 Experimental evaluation

In this section, we compare numerically SBS and its variants with the state-of-the-art global optimization methods: CMA-ES [12], WOA [28] (a particle-swarm method), ADALIPO [25], BAYESOPT [26], and a similar method to SBS but using MALA instead of SVGD [11, 30, 38]. We also provide a variant that uses SBS-PF as the final step of SBS-HYBRID, named SBS-PF-HYBRID. We use classical two dimensional benchmark functions for global optimization. Some are noisy and multimodal (Ackley, Drop wave, Egg Holder, Holder Table, Michalewicz, Rastrigin, Levy), others are smooth (Brannin, Goldstein Price, Himmelblau, Rosenbrock, Camel, Sphere) (see more information in [35]). We provide the implementation of this experiment¹. For the results of Tab. 1, we ran each method 10 times on each function. In the literature, the budget is defined as the number of function evaluations, however, the computational time can vary significantly between the methods and needs to be taken into account. Thus, the budget is set in order for the methods to stop in a reasonable time when run on a personal computer². As one can see in Fig. 4b, the running time of ADALIPO and BAYESOPT is significantly higher than for the other methods. For this reason, their budget is set lower than for the other methods: 2K for ADALIPO, 100 for BAYESOPT, and 800K for the rest.

Let us also introduce the following empirical *competitive ratio*:

$$CR(m) = \frac{1}{|F|} \sum_{f \in F} \min \left(100, \frac{df_m}{df^*} \right),$$

where F is the set of benchmark functions, df_m is the distance between the global minimum of f and the approximation found by the method m , and df^* is the smallest distance among all the methods. This measure provides information about the average precision compared to the best method (lower is better, and the best is 1).

In the results of Tab. 1, one can see that SBS outperforms the state-of-the-art methods and scores the third rank on average. SBS-PF achieves comparable results on average with significantly less function evaluations ($\sim 97\%$ budget reduction). Even if the asymptotic consistency is not guaranteed for SBS-PF, the particle filtering strategy allows to beat all SOTA methods except WOA, while using only a fraction of the available budget. Moreover, SBS-HYBRID and SBS-PF-HYBRID outperform all the other methods on average. They combine the efficiency of both CMA-ES and WOA with the large budget compatibility of SBS, while the addition of particle filtering reduces the budget by $\sim 67\%$. In parallel, SBS, SBS-PF-HYBRID, and SBS-HYBRID score respectively the 4th, 2nd, and 1st rank on the competitive ratio metric (CR), showing that their approximations are precise compared to the other methods. SBS and SBS-HYBRID succeed in beating CMA-ES and WOA while

¹github.com/gaetanserre/Stochastic-Global-Optimization

²The experiments were performed on an Apple M2 chip with 8 cores and 16GB of RAM.

being asymptotically consistent. In the appendix, we provide the results of the same experiment on 50 dimensional benchmark functions restricting to only methods that can run in low computational time (see Tab. 2). There, the budget is set to 8M. One can observe a fairly similar behavior as in the 2d case. However, the budget reduction of SBS-PF-HYBRID is less significant ($\sim 9\%$), due to the fact that the high dimensionality of the functions and the initial distribution makes the unpromising particles harder to distinguish. Overall, all SBS versions seem robust to any shape of function (in the contrary of CMA-ES for example, which is very precise on valley-shaped functions but struggles on multimodal ones). Moreover, SBS-PF-HYBRID is the best compromise in terms of precision and budget reduction.

6 Discussion

Link with Simulated Annealing. The link between SBS and Simulated Annealing [16] is not difficult to see. Indeed, both algorithms are asymptotic methods that sample from the BD. However, the way they sample from that distribution is different. Simulated Annealing is a Markov Chain Monte-Carlo method [2], while SBS is a deterministic variational approach. The minimum temperature parameter of Simulated Annealing is the inverse of the κ parameter of SBS. Thus, any scheduler for Simulated Annealing’s temperature can also be used in SBS. However, there is an extra degree of exploration/exploitation in SBS, brought by the kernel bandwidth employed by the SVGD sampling.

Locality of the kernel. In classical SVGD implementations, the used RBF kernel is: $k(x, x') = \exp(-\|x - x'\|_2^2 / 2\sigma^2)$, as it is in the Stein class of any smooth density supported on \mathbb{R}^d . The bandwidth σ controls the locality of the attraction and repulsion forces applied on the particles, respectively expressed as:

$$\begin{aligned} \text{attr}(x) &= \mathbb{E}_{x' \sim \hat{\mu}_i} [\nabla \log \pi(x') k(x, x')] , \\ \text{rep}(x) &= \mathbb{E}_{x' \sim \hat{\mu}_i} [\nabla_{x'} k(x, x')] . \end{aligned}$$

The first term attracts lonely particles to a close cluster of particles, and the second term repels particles that are too close to each other. They are respectively exploitation and exploration forces. Indeed, the attraction allows particles to “fall” in local minima, where a lot of particles are already stuck in. The repulsion prevents particles from getting stuck together at a narrow region of the search space, and forces them to explore the space. The value of σ controls the range of these forces. A small σ value leads to a weak repulsion and thus more exploitation. An arbitrary small σ leads to a uniform distribution over the local minima. In the contrary, a large σ leads to more exploration, as the particles will repel themselves from even from a very far distance. An arbitrary large σ leads to a uniform discretization of the space. In the case of SBS, the value of σ is not fixed and can be chosen by the user. These behaviors are illustrated in Fig. 5.

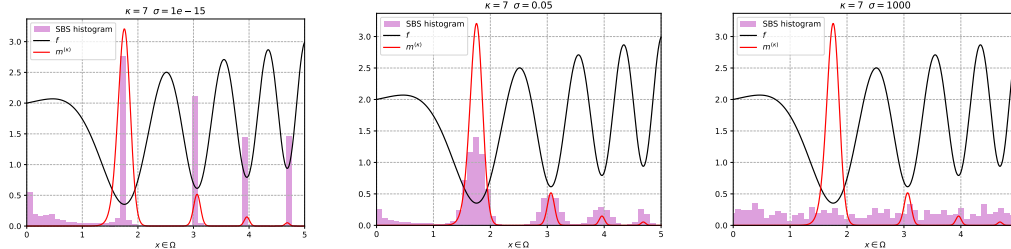


Figure 5. Illustration of the exploration/exploitation trade-off in SBS with different values of σ . In **black**, the function $x \mapsto \cos(x^2) + x/5 + 1$; in **violet**, the distribution of the particles; in **red**, the BD $m^{(\kappa)}$. When σ is too small, the particles are uniformly distributed over X^* . When σ is too large, they are uniformly distributed over the whole domain Ω .

7 Conclusion

In this paper, we introduced the Stein Boltzmann Sampling (SBS) method for global optimization. We proved that it is consistent using theory of the SVGD algorithm, that we extended to a more general class of target distributions, thanks to the compactness of the domain. This new SVGD framework is

particularly suitable for global optimization, as it allows to sample from the BD of any continuous function given integration constraints on its 1st order weak derivatives. We showed in our experimental evaluation that SBS outperforms state-of-the-art methods on average on classical benchmark functions, that SBS-PF can lead to drastic reduction of the needed computational budget while having comparable performance than the original SBS version, and that SBS-HYBRID outperforms all the other methods in practice. Our work suggests that, obtaining the best trade-off between accurate approximations and low budget, SBS should be used as a continuation for others particles or distribution-based methods, conjointly with particles filtering strategies (SBS-PF-HYBRID). In the future, we plan to study further the convergence rate of SBS and its components, and design more sophisticated particle filtering strategies to make it more appealing for global optimization in real-world applications.

References

- [1] Aronszajn, N. *Theory of Reproducing Kernels*. Transactions of the American Mathematical Society, 1950.
- [2] Azencott, R. Simulated annealing, 1989.
- [3] Billingsley, P. *Convergence of Probability Measures*. Wiley, 1999.
- [4] Bortoli, V. D. and Desolneux, A. On quantitative laplace-type convergence results for some exponential probability measures, with two applications, 2021.
- [5] Davis, D., Drusvyatskiy, D., Lee, Y. T., Padmanabhan, S., and Ye, G. A gradient sampling method with complexity guarantees for lipschitz functions in high and low dimensions. *Proceedings of Advances in Neural Information Processing Systems*, 2022.
- [6] de Moura, L. and Ullrich, S. The Lean 4 theorem prover and programming language. In *Automated Deduction – CADE 28*. Springer International Publishing, 2021.
- [7] Duncan, A., Nüsken, N., and Szpruch, L. On the geometry of stein variational gradient descent. *Journal of Machine Learning Research*, 2023.
- [8] Erdogdu, M. A., Mackey, L., and Shamir, O. Global non-convex optimization with discretized diffusions. *Advances in Neural Information Processing Systems*, 31, 2018.
- [9] Evans, L. C. and Gariepy, R. F. *Measure Theory and Fine Properties of Functions, Revised Edition*. Chapman and Hall/CRC, 2015.
- [10] Gorham, J. and Mackey, L. Measuring sample quality with stein’s method. *Proceedings of Advances in Neural Information Processing Systems*, 2015.
- [11] Grenander, U. and Miller, M. I. Representations of knowledge in complex systems. *Journal of the Royal Statistical Society. Series B (Methodological)*, 1994.
- [12] Hansen, N. and Ostermeier, A. Adapting arbitrary normal mutation distributions in evolution strategies: the covariance matrix adaptation. In *Proceedings of IEEE International Conference on Evolutionary Computation*, 1996.
- [13] Hwang, C.-R. Laplace’s Method Revisited: Weak Convergence of Probability Measures. *The Annals of Probability*, pp. 1177–1182, 1980.
- [14] Jordan, M. I., Kornowski, G., Lin, T., Shamir, O., and Zampetakis, M. Deterministic Nonsmooth Nonconvex Optimization, 2023.
- [15] Kingma, D. and Ba, J. Adam: A method for stochastic optimization. In *Proceedings of the International Conference on Learning Representations*, 2015.
- [16] Kirkpatrick, S., Gelatt, C. D., and Vecchi, M. P. Optimization by simulated annealing. *Science*, 1983.
- [17] Korba, A., Salim, A., Arbel, M., Luise, G., and Gretton, A. A non-asymptotic analysis for stein variational gradient descent. In *Proceedings of Advances in Neural Information Processing Systems*, 2020.
- [18] Korba, A., Aubin-Frankowski, P.-C., Majewski, S., and Ablin, P. Kernel stein discrepancy descent. In *Proceedings of the International Conference on Machine Learning*, 2021.
- [19] Lee, J., Lee, I.-H., Joung, I., Lee, J., and Brooks, B. R. Finding multiple reaction pathways via global optimization of action. *Nature Communications*, 2017.
- [20] Liu, Q. Stein variational gradient descent as gradient flow. *Proceedings of Advances in Neural Information Processing Systems*, 2017.
- [21] Liu, Q. and Wang, D. Stein variational gradient descent: A general purpose bayesian inference algorithm. *Proceedings of Advances in Neural Information Processing Systems*, 2016.
- [22] Liu, Q., Lee, J., and Jordan, M. A kernelized stein discrepancy for goodness-of-fit tests. In *Proceedings of the International Conference on Machine Learning*, 2016.

- [23] Lu, J., Lu, Y., and Nolen, J. Scaling limit of the stein variational gradient descent: The mean field regime. *SIAM Journal on Mathematical Analysis*, 2019.
- [24] Luo, X. Minima distribution for global optimization, 2019.
- [25] Malherbe, C. and Vayatis, N. Global optimization of Lipschitz functions. In *Proceedings of the International Conference on Machine Learning*, 2017.
- [26] Martinez-Cantin, R. Bayesopt: A bayesian optimization library for nonlinear optimization, experimental design and bandits. *Journal of Machine Learning Research*, 2014.
- [27] mathlib Community, T. The Lean mathematical library. In *Proceedings of the ACM SIGPLAN International Conference on Certified Programs and Proofs*, 2020.
- [28] Mirjalili, S. and Lewis, A. The whale optimization algorithm. *Advances in engineering software*, 2016.
- [29] Pintér, J. D. Global optimization in action. *Scientific American*, 1991.
- [30] Raginsky, M., Rakhlin, A., and Telgarsky, M. Non-convex learning via stochastic gradient langevin dynamics: a nonasymptotic analysis. In *Proceedings of the 2017 Conference on Learning Theory*, 2017.
- [31] Rudi, A., Marteau-Ferey, U., and Bach, F. Finding global minima via kernel approximations. *Mathematical Programming*, pp. 1–82, 2024.
- [32] Sriperumbudur, B. K., Fukumizu, K., and Lanckriet, G. R. G. Universality, Characteristic Kernels and RKHS Embedding of Measures. *Journal of Machine Learning Research*, 2011.
- [33] Stein, C. A bound for the error in the normal approximation to the distribution of a sum of dependent random variables. In *Proceedings of the Berkeley Symposium on Mathematical Statistics and Probability, Volume 2: Probability Theory*, 1972.
- [34] Sun, L., Karagulyan, A., and Richtarik, P. Convergence of stein variational gradient descent under a weaker smoothness condition. In *International Conference on Artificial Intelligence and Statistics*, 2023.
- [35] Surjanovic, S. and Bingham, D. Virtual library of simulation experiments: Test functions and datasets. Retrieved April 29, 2024, from <http://www.sfu.ca/~ssurjano>.
- [36] Villani, C. *Topics in Optimal Transportation*. Graduate studies in mathematics. American Mathematical Society, 2003.
- [37] Villani, C. *Optimal Transport*. Springer Berlin Heidelberg, 2009.
- [38] Welling, M. and Teh, Y. W. Bayesian learning via stochastic gradient langevin dynamics. In *Proceedings of the International Conference on Machine Learning*, 2011.
- [39] Zhang, J., Lin, H., Jegelka, S., Sra, S., and Jadbabaie, A. Complexity of finding stationary points of nonconvex nonsmooth functions. In *Proceedings of the International Conference on Machine Learning*, 2020.
- [40] Zhou, D.-X. Derivative reproducing properties for kernel methods in learning theory. *Journal of Computational and Applied Mathematics*, 2008.

Table 2. Comparative results. Comparison between all SBS variants with several state-of-the-art methods on 50 dimensional benchmark functions. For each function, we report the average best function value found (lower is better). SBS-HYBRID runs 1K iterations of CMA-ES and WOA. As one can see, SBS-HYBRID and SBS respectively rank 2nd and 4th while SBS-PF-HYBRID and SBS-PF achieve competitive results with less evaluations (respectively $\sim 9\%$ and $\sim 97\%$ budget reduction). The high dimensionality of the functions makes the particle filtering of SBS-PF-HYBRID less efficient.

FUNCTIONS	STATE-OF-THE-ART				PROPOSED METHODS			
	WOA	LANGEVIN	CMA-ES		SBS-PF	SBS	SBS-PF-HYBRID	SBS-HYBRID
ACKLEY	19.737	21.514	19.420		18.935	19.039	19.631	19.479
MICHALEWICZ	-13.663	-0.823	-34.069		-11.905	-13.626	-32.673	-32.556
RASTRIGIN	570.841	25.207	101.817		276.598	267.643	127.023	107.124
ROSEN BROCK	19021.088	0.254	3×10^{-14}		26.156	36.757	26.329	43.631
LEVY	215.674	2837.201	85.298		58.677	52.496	74.093	41.644
SPHERE	636.685	0.001	1×10^{-14}		1×10^{-4}	2×10^{-10}	9×10^{-23}	6×10^{-20}
COMP. RATIO	38.172	45.105	1.686		35.579	19.439	18.300	18.036
AVERAGE RANK	6.17	5.00	2.50		4.00	3.83	3.33	3.17
FINAL RANK	7	6	1		5	4	3	2

Appendix

Table 3. Collection of all notations and their meanings

Notation	Definition
f	function to minimize
d	dimension of the domain of f
Ω	compact subset of \mathbb{R}^d , domain of f
X^*	set of global minimizers of f
$W^{p,m}$	Sobolev space of functions with p -integrable m -th order weak derivatives
H^m	$W^{2,m}$
λ	Lebesgue measure
$m(\kappa)$	density of the BD with parameter κ
\mathcal{A}_μ	the Stein operator associated to the measure μ
$\mathcal{S}(\mu)$	the Stein class of the measure μ
$\mathcal{P}_2(\Omega)$	the set of probability measures supported over Ω with density in H^1
π	target distribution, the BD of f in SBS context
\mathcal{H}_0	the foundational RKHS of SVGD
k	the kernel of the RKHS \mathcal{H}_0
\mathcal{H}	the product RKHS of SVGD constructed using \mathcal{H}_0
T_μ	an integral operator from $L_\mu^2(\Omega)$ to \mathcal{H}_0
S_μ	an integral operator from $L_\mu^2(\Omega, \Omega)$ to \mathcal{H} constructed using T_μ
ϕ_μ^*	the optimal transport vector field in \mathcal{H} constructed by SVGD
$\mathfrak{K}(\mu \pi)$	the Kernelized Stein Discrepancy
$(\mu_i)_{i \in \mathbb{N}}$	sequence of measures constructed by SVGD
$\hat{\mu}_i$	empirical measure of the SVGD particles
$(\mu_t)_{t \in \mathbb{R}_{\geq 0}}$	net extension of $(\mu_i)_{i \in \mathbb{N}}$
$\Phi : \mathbb{R}_{\geq 0} \times \mathcal{P}_2(\Omega)$	the flow of measures associated to $(\mu_t)_{t \in \mathbb{R}_{\geq 0}}$

A Theoretical foundations

In this section, we introduce fundamental results related to the Boltzmann distribution (BD) and the SVGD theory. Please note that, concerning the BD, those results are not new. Concerning SVGD, we adapt its generic theoretical framework, allowing more general target distributions. We prove classical results of SVGD theory in this novel framework. The purpose of this section is to provide a self-contained presentation of the theory behind SBS for the reader and to show the consistency of our adapted SVGD framework.

A.1 Boltzmann distribution

Recall that the BD has been formally defined, in Definition 2.1. The BD is a well-known distribution in statistical physics. It is used to model the distribution of the energy of a system in thermal equilibrium. The parameter κ is called the *inverse temperature*. The higher κ is, the more concentrated the mass is around the minima of f . When κ tends to infinity, the BD tends to a distribution supported over the minima of f . The BD is typically used in a discrete settings, i.e. where the number of states is finite. The continuous version can be defined using the Gibbs measure. The following properties come from [24]. For the sake of completeness, we provide the proofs in Appendix B.1.

Properties A.1 (Properties of the Boltzmann distribution). Let $m^{(\kappa)}$ be defined as in Definition 2.1. Then, we have the following properties:

- If $\lambda(X^*) = 0$, then, $\forall x \in \Omega$,

$$\lim_{\kappa \rightarrow \infty} m^{(\kappa)}(x) = \begin{cases} \infty & \text{if } x \in X^* \\ 0 & \text{otherwise.} \end{cases}$$

- If $0 < \lambda(X^*)$, then, $\forall x \in \Omega$,

$$\lim_{\kappa \rightarrow \infty} m^{(\kappa)}(x) = \begin{cases} \lambda(X^*)^{-1} & \text{if } x \in X^* \\ 0 & \text{otherwise.} \end{cases}$$

- $\forall f \in C^0(\Omega, \mathbb{R})$,

$$\lim_{\kappa \rightarrow \infty} \int_{\Omega} f(x) m^{(\kappa)}(x) dx = f^*.$$

A visual representation of the BD is given in Fig. 2a. One can see that, as κ increases, $m^{(\kappa)}$ becomes more and more concentrated around the minima of f . We use the BD induced by the density $m^{(\kappa)}$ (also noted $m^{(\kappa)}$ for simplicity) of Eq. 2. We provide the proof of the properties in Appendix B.1. To sample from this distribution, we need to compute the integral $\int_{\Omega} e^{-\kappa f(t)} dt$, which however, is likely to be intractable for a general f .

A.2 Stein Variational Gradient Descent

Sampling from an intractable distribution is a common task in Bayesian inference, where the target distribution is a posterior one. Computation becomes difficult due to the presence of an intractable integral within the likelihood. The *Stein Variational Gradient Descent* [21] is a method that transforms iteratively an arbitrary measure μ to a target distribution π . In the case of SBS, π is the BD defined in Definition 2.1, for any $\kappa > 0$. The algorithm is based on the *Stein method* [33]. The theory of SVGD has been developed in several works over the years. Note that recently, [18] introduced a new sampling algorithm based on the same objective to SVGD, less sensitive to the choice of the step-size but not suitable for non-convex objectives. The remainder of this section introduces key definitions and theoretical results related to SVGD and shows that they hold when considering a compact domain Ω and a target distribution density in $H^1(\Omega)$: a adapted framework particularly suitable for global optimization that we use to prove the consistency of SBS (see Sec. 2.2).

A.2.1 Definitions

For any natural number n , we start by defining the set of probability measures on Ω that have a density w.r.t. the Lebesgue measure and are in $W^{1,n}(\Omega)$. Let $\mathcal{P}_n(\Omega)$ denote the set of probability measures on Ω such that

$$\forall \mu \in \mathcal{P}_n(\Omega), \mu \ll \lambda \wedge \mu(\cdot) \in W^{1,n}(\Omega) \wedge \text{supp}(\mu(\cdot)) = \Omega,$$

where $\mu(\cdot)$ is the density of μ w.r.t. λ . In SVGD theory, μ and π must belong to $\mathcal{P}_2(\Omega)$. Thus, their densities lie in $H^1(\Omega)$. The condition on their support ensures that the KL divergence is well-defined. In the following, we denote the density w.r.t. λ of an arbitrary measure μ by the function $\mu : \Omega \rightarrow \mathbb{R}_{\geq 0}$.

A.2.2 Stein discrepancy

The Stein method defines the Stein operator associated to a measure μ [20]:

$$\begin{aligned} \mathcal{A}_\mu : C^1(\Omega, \Omega) &\rightarrow C^0(\Omega, \mathbb{R}), \\ \phi &\mapsto \nabla \log \mu(\cdot)^\top \phi(\cdot) + \nabla \cdot \phi(\cdot), \end{aligned}$$

where (∇) and $(\nabla \cdot)$ are respectively the gradient and the divergence operators, in the sense of distributions. We denote this mapping by $\mathcal{A}_\mu \phi$, for any ϕ in $C^1(\Omega, \Omega)$. It also defines a class of functions, the Stein class of measures.

Definition A.2 (Stein class of measures [22]). Let $\mu \in \mathcal{P}_2(\Omega)$ such that $\mu \ll \lambda$, and let $\phi : \Omega \rightarrow \Omega$. As Ω is compact, the boundary of Ω (denoted by $\partial\Omega$) is nonempty. We say that ϕ is in the *Stein class* of μ if $\phi \in H^1(\Omega)$ and

$$\oint_{\partial\Omega} \mu(x) \phi(x) \cdot \vec{n}(x) \, dS(x) = 0,$$

where $\vec{n}(x)$ is the unit normal vector to the boundary of Ω . We denote by $\mathcal{S}(\mu)$ the Stein class of μ .

The key property of $\mathcal{S}(\mu)$ is that, for any function f in $\mathcal{S}(\mu)$, the expectation of $\mathcal{A}_\mu f$ w.r.t. μ is null.

Lemma A.3 (Stein identity [33]). Let $\mu \in \mathcal{P}_2(\Omega)$ such that $\mu \ll \lambda$, and let $\phi \in \mathcal{S}(\mu)$. Then,

$$\mathbb{E}_{x \sim \mu} [\mathcal{A}_\mu \phi(x)] = 0.$$

(See proof in Appendix B.3). Now, one can consider:

$$\mathbb{E}_{x \sim \mu} [\mathcal{A}_\pi \phi(x)], \text{ where } \phi \in \mathcal{S}(\pi). \quad (5)$$

If $\mu \neq \pi$, Eq. 5 would no longer be null for any ϕ in $\mathcal{S}(\pi)$. In fact, the magnitude of this expectation relates to how different μ and π are, and is used to define a discrepancy measure, known as the *Stein discrepancy* [10]. The latter considers the “maximum violation of Stein’s identity” given a proper set of functions $\mathcal{F} \subseteq \mathcal{S}(\pi)$:

$$\mathbb{S}(\mu, \pi) = \max_{\phi \in \mathcal{F}} \{ \mathbb{E}_{x \sim \mu} [\mathcal{A}_\pi \phi(x)] \}. \quad (6)$$

Note that $\mathbb{S}(\mu, \pi)$ is not symmetric. The set $\mathcal{S}(\pi)$ might be different to $\mathcal{S}(\mu)$, and even if they are equal, inverting the densities in the expectation leads to a different result. The choice of \mathcal{F} is crucial as it determines the discriminative power and tractability of the Stein discrepancy. It also has to be included in $\mathcal{S}(\pi)$. Traditionally, \mathcal{F} is chosen to be the set of all functions with bounded Lipschitz norms, but this choice casts a challenging functional optimization problem. To overcome this difficulty, [22] chose \mathcal{F} to be a universal vector-valued RKHS, which allows to find closed-form solution to Eq. 6. The Stein discrepancy restricted to that RKHS is known as *Kernelized Stein Discrepancy*.

A.2.3 Kernelized Stein Discrepancy

From now on, we consider $\mu, \pi \in \mathcal{P}_2(\Omega)$ such that π is the target distribution. Next, we define the vector-valued RKHS that will be used in the Kernelized Stein Discrepancy.

Definition A.4 (Product RKHS [21]). Let $k : \Omega \times \Omega \rightarrow \mathbb{R}$ be a continuous, symmetric, and integrally positive-definite kernel such that $\forall x \in \Omega, k(\cdot, x) \in \mathcal{S}(\mu) \cap \mathcal{S}(\pi)$ and $\nabla_{xy} k(x, y) \in L_\mu^2(\Omega)$ (in the sense of distributions). Using the Moore–Aronszajn theorem [1], we consider the associated real-valued RKHS \mathcal{H}_0 . Let \mathcal{H} be the product RKHS induced by \mathcal{H}_0 , i.e. $\forall f = (f_1, \dots, f_d)^\top$, $f \in \mathcal{H} \iff \forall 1 \leq i \leq d, f_i \in \mathcal{H}_0$. The inner product of \mathcal{H} is defined by

$$\langle f, g \rangle_{\mathcal{H}} = \sum_{1 \leq i \leq d} \langle f_i, g_i \rangle_{\mathcal{H}_0}.$$

For more details, see Lean formalization³.

Let $L_\mu^2(\Omega)$ be the set of functions from Ω to \mathbb{R} that are square-integrable w.r.t. μ . Let $L_\mu^2(\Omega, \Omega)$ be the set of functions from Ω to Ω that are component-wise in $L_\mu^2(\Omega)$, i.e.

$$\forall f \in L_\mu^2(\Omega, \Omega), \forall 1 \leq i \leq d, f_i \in L_\mu^2(\Omega).$$

³gaetanerre.fr/assets/Lean/SBS/html/RKHS.lean.html

As k is integrally positive-definite, \mathcal{H}_0 is dense in $L_\mu^2(\Omega)$ (see [32]), which shows its expressiveness. We proved that the integral operator

$$T_\mu : L_\mu^2(\Omega) \rightarrow L_\mu^2(\Omega)$$

$$f \mapsto \int_\Omega k(\cdot, x)f(x) d\mu(x)$$

is a mapping from $L_\mu^2(\Omega)$ to \mathcal{H}_0 , i.e. $T_\mu : L_\mu^2(\Omega) \rightarrow \mathcal{H}_0$. (See proof in Appendix B.4). This allows to define another integral operator

$$S_\mu : L_\mu^2(\Omega, \Omega) \rightarrow \mathcal{H}$$

$$f \mapsto (T_\mu f^{(1)}, \dots, T_\mu f^{(d)})^\top,$$

where T_μ is applied component-wise. The proof in Appendix B.4 also shows that \mathcal{H} is a subset of $L_\mu^2(\Omega, \Omega)$. Thus, we can define the inclusion map

$$\iota : \mathcal{H} \hookrightarrow L_\mu^2(\Omega, \Omega),$$

whose adjoint is $\iota^* = S_\mu$. Then, have the following equality:

$$\forall f \in L_\mu^2(\Omega, \Omega), \forall g \in \mathcal{H},$$

$$\langle f, \iota g \rangle_{L_\mu^2(\Omega, \Omega)} = \langle \iota^* f, g \rangle_{\mathcal{H}} = \langle S_\mu f, g \rangle_{\mathcal{H}}.$$

We can now define the KSD.

Definition A.5 (Kernelized Stein Discrepancy [22]). Let \mathcal{H} be a product RKHS as defined in Definition A.4. The *Kernelized Stein Discrepancy* (KSD) is then defined as:

$$\mathfrak{K}(\mu|\pi) = \max_{f \in \mathcal{H}} \{ \mathbb{E}_{x \sim \mu} [\mathcal{A}_\pi f(x)] \mid \|f\|_{\mathcal{H}} \leq 1 \}.$$

The construction of \mathcal{H} was motivated by the fact that the closed-form solution of the KSD is given by the following theorem.

Theorem A.6 (Steepest trajectory [22]). *The function that maximizes the KSD is given by:*

$$\frac{\phi_\mu^*}{\|\phi_\mu^*\|_{\mathcal{H}}} = \arg \max_{f \in \mathcal{H}} \{ \mathbb{E}_{x \sim \mu} [\mathcal{A}_\pi f(x)] \mid \|f\|_{\mathcal{H}} \leq 1 \}.$$

where $\phi_\mu^* = \mathbb{E}_{x \sim \mu} [\nabla \log \pi(x) k(\cdot, x) + \nabla_x k(\cdot, x)]$. As $\text{supp}(\pi) = \Omega$, ϕ_μ^* is well-defined. It is the steepest trajectory in \mathcal{H} that maximizes $\mathfrak{K}(\mu|\pi)$. The KSD is then given by

$$\mathfrak{K}(\mu|\pi) = \mathbb{E}_{x \sim \mu} [\mathcal{A}_\pi \phi_\mu^*(x)].$$

The proof strategy is to remark that, for any function $f \in \mathcal{H}$, $\mathbb{E}_{x \sim \mu} [\mathcal{A}_\pi f(x)] = \langle f, \phi_\mu^* \rangle_{\mathcal{H}}$. Then, the result follows from the Cauchy-Schwarz inequality. (See proof in Appendix B.5). This leads to the following result of the SVGD theory.

Theorem A.7 (KL steepest descent trajectory [21]). *Let \mathcal{H} be a product RKHS (Definition A.4). Let $\phi_\mu^* \in \mathcal{H}$ be as defined in Theorem A.6. Let $\varepsilon > 0$ and*

$$T_\varepsilon : (\Omega \rightarrow \Omega) \rightarrow \Omega$$

$$\phi \mapsto I_d + \varepsilon \phi.$$

Then,

$$\arg \min_{\phi \in \mathcal{H}} \{ \nabla_\varepsilon \text{KL}(T_\varepsilon(\phi)_{\#} \mu | \pi) |_{\varepsilon=0} \mid \|\phi\|_{\mathcal{H}} \leq 1 \} = \frac{\phi_\mu^*}{\|\phi_\mu^*\|_{\mathcal{H}}},$$

and $\nabla_\varepsilon \text{KL}((I_d + \varepsilon \phi_\mu^*)_{\#} \mu | \pi) |_{\varepsilon=0} = -\mathfrak{K}(\mu|\pi)$.

(See proof in Appendix B.6). This last result is the key of the SVGD algorithm. It means that ϕ_μ^* is the optimal direction (within \mathcal{H}) to update μ in order to minimize the KL-divergence between μ and π . As $\mathbf{0} \in \mathcal{H}$ (that nullifies the gradient), the result ensures that the gradient of $g : \varepsilon \mapsto \text{KL}(T_\varepsilon(\phi_\mu^*/\|\phi_\mu^*\|_{\mathcal{H}})_{\#} \mu | \pi)$ is at most 0 and thus g is decreasing over $[0, \delta]$, for $\delta > 0$ small enough. Consequently, SVGD iteratively updates μ in the direction induced by ϕ_μ^* , with a small step size ε :

$$\mu_{i+1} = (I_d + \varepsilon \phi_{\mu_i}^*)_{\#} \mu_i. \quad (7)$$

Furthermore, given the above assumption on ϕ_μ^* , we have the following lemma.

Lemma A.8. *Let \mathcal{H} be a product RKHS as defined in Definition A.4. Then, $\phi_\mu^* \in \mathcal{H}$ as defined in Theorem A.6. Given the above assumption on ϕ_μ^* , we have that*

$$\mathfrak{R}(\mu|\pi) = \|\phi_\mu^*\|_{\mathcal{H}}^2.$$

Proof. We showed in Appendix B.5 that

$$\mathbb{E}_{x \sim \mu}[\mathcal{A}_\pi f(x)] = \langle f, \phi_\mu^* \rangle_{\mathcal{H}}$$

for any $f \in \mathcal{H}$. Thus, $\mathbb{E}_{x \sim \mu}[\mathcal{A}_\pi \phi_\mu^*(x)] = \langle \phi_\mu^*, \phi_\mu^* \rangle_{\mathcal{H}}$. ■

In particular, this lemma states that the derivative of the KL-divergence when considering the direction ϕ_μ^* is negative, meaning that the sequence $(\text{KL}(\mu_i|\pi))_{i \in \mathbb{N}}$ is decreasing, given that the step size is small enough. In order to use theorems in Sec. 2.2, we need to ensure that

$$\phi_\mu^* \in \mathcal{S}(\mu).$$

Given the assumption of the kernel, ϕ_μ^* lies in $H^1(\Omega)$. Thus, we need to choose k in order to ensure that the integral of ϕ_μ^* over $\partial\Omega$ is null. An easy way to guarantee this is to choose k such that

$$\begin{aligned} \forall x \in \Omega, \quad \lim_{d(\{y\}, \partial\Omega) \rightarrow 0} \nabla_x k(y, x) &= 0, \text{ and} \\ \lim_{d(\{y\}, \partial\Omega) \rightarrow 0} \nabla \log \pi(x) k(y, x) &= 0, \text{ where} \\ d(A, B) &= \inf \{\|a - b\|_2 \mid a \in A \wedge b \in B\}. \end{aligned}$$

This would be the case for a modified Gaussian kernel:

$$k(x, y) = \exp\left(-\frac{\|x - y\|_2^2}{2\sigma^2 f(x, y)}\right),$$

where f is a positive and symmetric function such that f and its gradient w.r.t. x tend to 0 near the boundary of Ω sufficiently fast to ensure the previous conditions. This assumption allows to use Lemma A.3 with ϕ_μ^* , for any $\mu \in \mathcal{P}_2(\Omega)$.

B Proofs

In the following sections, we provide the proofs of the theorems and lemmas stated in the main text. We also provide Lean proofs of some results. The Lean proofs are available here⁴. Note that a collection of all key notations and their meanings is available in Tab. 3. We also introduce a new quantifier $\bar{\forall}_\mu$, such that, given a predicate P and a measure μ ,

$$\bar{\forall}_\mu x \in E \subseteq \Omega, P(x) \triangleq \mu(\{x \in E \mid \neg P(x)\}) = 0.$$

This quantifier means that the predicate P is true for almost all $x \in E$ w.r.t. the measure μ . When the considered measure is the standard Lebesgue measure, we simply write $\bar{\forall}$. This quantifier can be found in Lean, noted $\forall^m \cdot \partial\mu$.

B.1 Proof of Properties A.1

The continuous BD is a special case of the nascent minima distribution, introduced in [24], that has the generic form

$$m_{f, \Omega}^{(\kappa)}(x) = m^{(\kappa)}(x) = \frac{\tau^\kappa(f(x))}{\int_\Omega \tau^\kappa(f(t)) \, dt}, \quad (8)$$

where $\tau : \mathbb{R} \rightarrow \mathbb{R}_{>0}$ is monotonically decreasing. We have the following theorems for general τ .

Theorem B.1 (Nascent minima distribution properties). *Let $m^{(\kappa)}$ and τ be defined in Eq. 8. Then, we have the following properties:*

⁴gaetanerre.fr/assets/Lean/SBS/index.html

- If $\lambda(X^*) = 0$, then, $\forall x \in \Omega$,

$$\lim_{\kappa \rightarrow \infty} m^{(\kappa)}(x) = \begin{cases} \infty & \text{if } x \in X^* \\ 0 & \text{otherwise} \end{cases}.$$

- If $0 < \lambda(X^*)$, then, $\forall x \in \Omega$,

$$\lim_{\kappa \rightarrow \infty} m^{(\kappa)}(x) = \begin{cases} \lambda(X^*)^{-1} & \text{if } x \in X^* \\ 0 & \text{otherwise} \end{cases}.$$

Proof. Let's prove the two properties together. Let $p = \tau(f(x')) > 0$, $\forall x' \notin X^*$. Then, $\exists \Omega_p$, such that $0 < \lambda(\Omega_p)$, $p < \tau(f(t))$, i.e. $f(t) < f(x')$. Thus,

$$\begin{aligned} m^{(\kappa)}(x') &= \frac{p^\kappa}{\int_{\Omega_p} \tau^\kappa(f(t)) \, dt + \int_{\Omega/\Omega_p} \tau^\kappa(f(t)) \, dt} \\ &\leq \frac{p^\kappa}{\int_{\Omega_p} \tau^\kappa(f(t)) \, dt} \\ &= \frac{1}{\int_{\Omega_p} p^{-\kappa} \tau^\kappa(f(t)) \, dt}. \end{aligned}$$

For any t in Ω_p , $p^{-1} \tau(f(t)) > 1$. Therefore $\lim_{\kappa \rightarrow \infty} \int_{\Omega_p} p^{-\kappa} \tau^\kappa(f(t)) \, dt = \infty$. Hence,

$$\forall x' \notin X^*, \lim_{\kappa \rightarrow \infty} m^{(\kappa)}(x) = 0.$$

Now, let's consider any $x'' \in X^*$ and $p = \tau(f(x''))$. We have

$$\begin{aligned} m^{(\kappa)}(x'') &= \frac{p^\kappa}{\int_{\Omega} \tau^\kappa(f(t)) \, dt} \\ &= \frac{1}{\int_{X^*} p^{-\kappa} \tau^\kappa(f(t)) \, dt + \int_{\Omega/X^*} p^{-\kappa} \tau^\kappa(f(t)) \, dt} \\ &= \frac{1}{\int_{X^*} dt + \int_{\Omega/X^*} p^{-\kappa} \tau^\kappa(f(t)) \, dt} \quad (\forall t \in X^*, \tau(f(t)) = p) \\ &= \frac{1}{\lambda(X^*) + \int_{\Omega/X^*} p^{-\kappa} \tau^\kappa(f(t)) \, dt}. \end{aligned}$$

For any t in Ω/X^* , $p^{-1} \tau(f(t)) < 1$. Therefore, $\lim_{\kappa \rightarrow \infty} \int_{\Omega/X^*} p^{-\kappa} \tau^\kappa(f(t)) \, dt = 0$. Thus,

$$\forall x'' \in X^*, \lim_{\kappa \rightarrow \infty} m^{(\kappa)}(x'') = \begin{cases} \infty & \text{if } \lambda(X^*) = 0 \\ \frac{1}{\lambda(X^*)} & \text{otherwise} \end{cases}.$$

■

Theorem B.2 (Convergence of expectation). $\forall f \in C^0(\Omega, \mathbb{R})$, the following holds

$$\lim_{\kappa \rightarrow \infty} \int_{\Omega} f(x) m^{(\kappa)}(x) \, dx = f^*.$$

Moreover, if $X^* = x^*$, we have

$$\lim_{\kappa \rightarrow \infty} \int_{\Omega} x m^{(\kappa)}(x) \, dx = x^*.$$

Proof. If f is constant, it is straightforward as $m^{(\kappa)}$ is a PDF. Suppose f not constant on Ω . For any $\varepsilon > 0$, let $0 < \delta \triangleq \frac{\varepsilon}{1 + (\max_{x \in \Omega} f(x) - f^*)} \leq \varepsilon$. As f is continuous, $\exists \Omega_\delta = \{x \in \Omega \mid f(x) - f^* < \delta\}$, the corresponding level set. Using Theorem B.1, $\exists K \in \mathbb{N}$ such that

$$\int_{\Omega/\Omega_\delta} m^{(\kappa)}(x) \, dx < \delta$$

holds $\forall \kappa > K$, as $m^{(\kappa)}$ tends to 0 $\forall x \notin X^*$. Thus,

$$\begin{aligned}
0 &< \int_{\Omega} f(x) m^{(\kappa)}(x) \, dx - f^* \\
&= \int_{\Omega} f(x) m^{(\kappa)}(x) \, dx - f^* \int_{\Omega} m^{(\kappa)}(x) \, dx \\
&= \int_{\Omega} (f(x) - f^*) m^{(\kappa)}(x) \, dx \\
&= \int_{\Omega_{\delta}} (f(x) - f^*) m^{(\kappa)}(x) \, dx \\
&\quad + \int_{\Omega/\Omega_{\delta}} (f(x) - f^*) m^{(\kappa)}(x) \, dx \\
&< \delta \int_{\Omega_{\delta}} m^{(\kappa)}(x) \, dx \\
&\quad + \left(\max_{x \in \Omega} f(x) - f^* \right) \int_{\Omega/\Omega_{\delta}} m^{(\kappa)}(x) \, dx \\
&< \delta(1 - \delta) + \left(\max_{x \in \Omega} f(x) - f^* \right) \delta \\
&< (1 + \left(\max_{x \in \Omega} f(x) - f^* \right)) \delta = \varepsilon.
\end{aligned}$$

The proof is similar for the second statement, by setting

$$\Omega_{\delta} = \{x \in \Omega \mid \|x - x^*\| < \delta\}.$$

■

Letting $\tau = x \mapsto e^{-x}$ gives Properties [A.1](#).

B.2 Proof of $f \in C^0(\Omega) \cap W^{1,4}(\Omega) \implies m^{(\kappa)} \in H^1(\Omega)$

Proof. As f and $\exp(\cdot)$ lie in $C^0(\Omega)$, $e^{-\kappa f}$ is also in $C^0(\Omega)$. As Ω is compact, $e^{-2\kappa f}$ is bounded. Thus, $e^{-\kappa f}$ lies in $L^2(\Omega)$:

$$\int_{\Omega} e^{-2\kappa f(x)} \, dx < \lambda(\Omega) * C < \infty.$$

Moreover, $\forall \alpha \in \mathbb{N}^d$ such that $|\alpha| \leq 1$, we have

$$D^{\alpha}(e^{-\kappa f}) = -\kappa e^{-\kappa f} D^{\alpha} f.$$

As f is in $W^{1,4}(\Omega)$, $D^{\alpha} f$ is in $L^4(\Omega)$. Thus, $D^{\alpha}(e^{-\kappa f})$ is also in $L^2(\Omega)$:

$$\begin{aligned}
\int_{\Omega} \left(D^{\alpha}(e^{-\kappa f(x)}) \right)^2 \, dx &= \int_{\Omega} -\kappa e^{-2\kappa f(x)} (D^{\alpha} f(x))^2 \, dx \\
&= \langle -\kappa e^{-\kappa f}, (D^{\alpha} f)^2 \rangle_{L^2(\Omega)} \\
&\leq \|-\kappa e^{-2\kappa f}\|_{L^2(\Omega)} \left\| (D^{\alpha} f)^2 \right\|_{L^2(\Omega)} \\
&= \|-\kappa e^{-2\kappa f}\|_{L^2(\Omega)} \|D^{\alpha} f\|_{L^4(\Omega)}^2 \\
&< \infty.
\end{aligned}$$

■

B.3 Proof of Lemma A.3.

Proof. As $\mu(\cdot)$ and ϕ are in $H^1(\Omega)$, and as Ω is smooth, one can apply the integration by parts formula in $\Omega \subset \mathbb{R}^d$ (see [9]):

$$\begin{aligned}\mathbb{E}_{x \sim \mu}[\mathcal{A}_\mu \phi(x)] &= \int_{\Omega} \nabla \log \mu(x)^\top \phi(x) + \nabla \cdot \phi(x) \, d\mu(x) \\ &= \int_{\Omega} \mu(x) (\nabla \log \mu(x)^\top \phi(x)) \, dx + \int_{\Omega} \mu(x) (\nabla \cdot \phi(x)) \, dx \\ &= \int_{\Omega} \mu(x) (\nabla \log \mu(x)^\top \phi(x)) \, dx - \int_{\Omega} \nabla \mu(x)^\top \phi(x) \, dx \\ &= \int_{\Omega} \nabla \mu(x)^\top \phi(x) \, dx - \int_{\Omega} \nabla \mu(x)^\top \phi(x) \, dx \\ &= 0.\end{aligned}$$

■

B.4 Proof of T_μ is a map to \mathcal{H}_0

Proof. As k is continuous, symmetric, and positive-definite and as $\mu(\Omega) < \infty$ and as T_μ is a self-adjoint operator, we can apply the Mercer's theorem to obtain a sequence of eigenfunctions $(\phi_i)_{i \in \mathbb{N}}$ and a sequence of eigenvalues $(\lambda_i)_{i \in \mathbb{N}}$ such that $(\phi_i)_{i \in I}$ is an orthonormal basis of $L_\mu^2(\Omega)$, such that $(\lambda_i)_{i \in \mathbb{N}}$ is nonnegative and converges to 0, and such that the following holds:

$$\forall s, t \in \Omega, k(s, t) = \sum_{i=1}^{\infty} \lambda_i \phi_i(s) \phi_i(t).$$

The above series converges absolutely and uniformly on $\Omega \times \Omega$. Let define the set

$$\mathcal{H}_k = \left\{ f \in L_\mu^2(\Omega) \left| f = \sum_{i=1}^{\infty} \lambda_i a_i \phi_i \wedge \sum_{i=1}^{\infty} \lambda_i a_i^2 < \infty \right. \right\},$$

endowed with the inner product

$$\forall f, g \in \mathcal{H}_k, \langle f, g \rangle_{\mathcal{H}_k} = \left\langle \sum_{i=1}^{\infty} \lambda_i a_i \phi_i, \sum_{i=1}^{\infty} \lambda_i b_i \phi_i \right\rangle_{\mathcal{H}_k} = \sum_{i=1}^{\infty} \lambda_i a_i b_i. \quad (9)$$

Routine works show that Eq. 9 defines a inner product and therefore that \mathcal{H}_k is a Hilbert space. Let's show that \mathcal{H}_k is a RKHS with kernel k , i.e., $\forall t \in \Omega, k(t, \cdot) \in \mathcal{H}_k$ and, $\forall f \in \mathcal{H}_k, f(t) = \langle f, k(t, \cdot) \rangle_{\mathcal{H}_k}$. Let $t \in \Omega$. First, Ω is compact, $\mu(\Omega) = 1 < \infty$, and $k(t, \cdot)$ is continuous on Ω , thus $k(t, \cdot) \in L_\mu^2(\Omega)$. Then, we have that

$$k(t, \cdot) = \sum_{i=1}^{\infty} \lambda_i \phi_i(t) \phi_i,$$

and

$$\sum_{i=1}^{\infty} \lambda_i \phi_i^2(t) = k(t, t) < \infty.$$

Thus, $k(t, \cdot) \in \mathcal{H}_k$. Let $f \in \mathcal{H}_k$. One can write

$$\begin{aligned}\langle f, k(t, \cdot) \rangle_{\mathcal{H}_k} &= \left\langle \sum_{i=1}^{\infty} \lambda_i a_i \phi_i, \sum_{i=1}^{\infty} \lambda_i \phi_i(t) \phi_i \right\rangle_{\mathcal{H}_k} \\ &= \sum_{i=1}^{\infty} \lambda_i a_i \phi_i(t) \\ &= f(t).\end{aligned}$$

Therefore, \mathcal{H}_k is indeed a RKHS with kernel k (for more details, see Lean proof ⁵) The Moore–Aronszajn theorem ensures that, given k , there exists a unique RKHS such that k is its kernel. Thus, $\mathcal{H}_k = \mathcal{H}_0$. That's prove that $\mathcal{H}_0 \subseteq L_\mu^2(\Omega)$, and thus $\mathcal{H} \subseteq L_\mu^2(\Omega, \Omega)$. Let's now prove that $\forall f \in L_\mu^2(\Omega)$, $T_\mu f \in \mathcal{H}_0$. Let $f \in L_\mu^2(\Omega)$. We begin by proving that $T_\mu f \in L_\mu^2(\Omega)$.

$$\begin{aligned} |T_\mu f(t)| &= \left| \int_{\Omega} k(t, s) f(s) \, d\mu(s) \right| \\ &\leq \int_{\Omega} |k(t, s)| |f(s)| \, d\mu(s) \\ &= \langle |k(t, \cdot)|, |f| \rangle_{L_\mu^2(\Omega)} \\ &\leq \|k(t, \cdot)\|_{L_\mu^2(\Omega)} \|f\|_{L_\mu^2(\Omega)}. \end{aligned}$$

Then,

$$\begin{aligned} \|T_\mu f(t)\|_{L_\mu^2(\Omega)}^2 &= \int_{\Omega} |T_\mu f(t)|^2 \, dt \\ &\leq \int_{\Omega} \|k(t, \cdot)\|_{L_\mu^2(\Omega)}^2 \, dt \|f\|_{L_\mu^2(\Omega)}^2 \\ &= \|k\|_{L_\mu^2}^2 \|f\|_{L_\mu^2(\Omega)}^2 \\ &< \infty. \end{aligned}$$

We now prove that $T_\mu f \in \mathcal{H}_0$.

$$\begin{aligned} T_\mu f &= \int_{\Omega} k(\cdot, s) f(s) \, d\mu(s) \\ &= \int_{\Omega} \sum_{i=1}^{\infty} \lambda_i f(s) \phi_i(s) \phi_i(\cdot) \, d\mu(s) \\ &= \sum_{i=1}^{\infty} \lambda_i \phi_i(\cdot) \int_{\Omega} f(s) \phi_i(s) \, d\mu(s) \\ &= \sum_{i=1}^{\infty} \lambda_i \langle f, \phi_i \rangle_{L_\mu^2(\Omega)} \phi_i. \end{aligned}$$

As $(\phi_i)_{i \in \mathbb{N}}$ is an orthonormal basis of $L_\mu^2(\Omega)$ we have that

$$\int_{\Omega} \phi_i \phi_j \, d\mu = \mathbb{1}_{\{i=j\}},$$

which implies, using Parseval's identity,

$$\sum_{i=1}^{\infty} \langle f, \phi_i \rangle_{L_\mu^2(\Omega)}^2 = \|f\|_{L_\mu^2(\Omega)}^2 < \infty.$$

As $(\lambda_i)_{i \in \mathbb{N}}$ converges to 0, $\exists I \in \mathbb{N}$ such that $\forall i > I$, $\lambda_i < 1$. Thus,

$$\begin{aligned} \sum_{i=1}^{\infty} \lambda_i \langle f, \phi_i \rangle_{L_\mu^2(\Omega)}^2 &= \sum_{i=1}^I \lambda_i \langle f, \phi_i \rangle_{L_\mu^2(\Omega)}^2 + \sum_{i=I+1}^{\infty} \lambda_i \langle f, \phi_i \rangle_{L_\mu^2(\Omega)}^2 \\ &\leq \sum_{i=1}^I \lambda_i \langle f, \phi_i \rangle_{L_\mu^2(\Omega)}^2 + \sum_{i=I+1}^{\infty} \langle f, \phi_i \rangle_{L_\mu^2(\Omega)}^2 \\ &\leq \sum_{i=1}^I \lambda_i \langle f, \phi_i \rangle_{L_\mu^2(\Omega)}^2 + \|f\|_{L_\mu^2(\Omega)}^2 \\ &< \infty. \end{aligned}$$

Therefore, $\forall f \in L_\mu^2(\Omega)$, $T_\mu f \in \mathcal{H}_0$, which proves that $T_\mu : L_\mu^2(\Omega) \hookrightarrow \mathcal{H}_0$. ■

⁵gaetan-serre.fr/assets/Lean/SBS/html/Inner.lean.html

B.5 Proof of Theorem A.6

Proof. First, we show that $\phi_\mu^* \in \mathcal{H}$, i.e. $\forall 1 \leq i \leq d, (\phi_\mu^*)^{(i)} \in \mathcal{H}_0$. Let define the function

$$\begin{aligned} f^{(i)} : \Omega &\rightarrow \mathbb{R}, \\ x &\mapsto \frac{\partial \log \frac{\pi}{\mu}(x)}{\partial x_i}. \end{aligned}$$

As $\text{supp}(\mu) = \Omega$, $f^{(i)}$ is well-defined and, as π and μ are in $H^1(\Omega)$, $f^{(i)}$ is in $L^2(\Omega)$. Then, as $\forall x \in \Omega, k(\cdot, x) \in \mathcal{S}(\mu)$, it is easy to show that

$$(\phi_\mu^*)^{(i)} = T_\mu f^{(i)} \in \mathcal{H}_0.$$

Thus, $\phi_\mu^* = S_\mu \nabla \log \frac{\pi}{\mu} \in \mathcal{H}$. Next, we prove that

$$\forall f \in \mathcal{H}, \mathbb{E}_{x \sim \mu} [\mathcal{A}_\pi f(x)] = \langle f, \phi_\mu^* \rangle_{\mathcal{H}}.$$

$$\begin{aligned} \langle f, \phi_\mu^* \rangle_{\mathcal{H}} &= \sum_{\ell=1}^d \left\langle f^{(\ell)}, \mathbb{E}_{x \sim \mu} \left[\nabla \log \pi^{(\ell)}(x) k(x, \cdot) + \nabla_x k^{(\ell)}(x, \cdot) \right] \right\rangle_{\mathcal{H}_0} \\ &= \mathbb{E}_{x \sim \mu} \left[\sum_{\ell=1}^d \langle f^{(\ell)}, \nabla \log \pi^{(\ell)}(x) k(\cdot, x) + \nabla_x k^{(\ell)}(x, \cdot) \rangle_{\mathcal{H}_0} \right] \\ &= \mathbb{E}_{x \sim \mu} \left[\sum_{\ell=1}^d \nabla \log \pi^{(\ell)}(x) \langle f^{(\ell)}, k(\cdot, x) \rangle_{\mathcal{H}_0} + \langle f^{(\ell)}, \nabla_x k^{(\ell)}(x, \cdot) \rangle_{\mathcal{H}_0} \right] \\ &= \mathbb{E}_{x \sim \mu} \left[\sum_{\ell=1}^d \nabla \log \pi^{(\ell)}(x) f^{(\ell)}(x) + \frac{\partial f^{(\ell)}(x)}{\partial x_\ell} \right] \quad [40] \\ &= \mathbb{E}_{x \sim \mu} \left[\nabla \log \pi(x)^\top f(x) + \nabla \cdot f(x) \right]. \end{aligned}$$

Moreover, using the Cauchy-Schwarz inequality, we have that

$$\langle f, \phi_\mu^* \rangle_{\mathcal{H}} \leq \|f\|_{\mathcal{H}} \|\phi_\mu^*\|_{\mathcal{H}}.$$

Thus, as $\|f\|_{\mathcal{H}} \leq 1$,

$$\mathfrak{R}(\mu, \pi) \leq \|\phi_\mu^*\|_{\mathcal{H}}.$$

Finally, by letting $f = \frac{\phi_\mu^*}{\|\phi_\mu^*\|_{\mathcal{H}}}$, we have that

$$\mathbb{E}_{x \sim \mu} [\mathcal{A}_\pi f] = \langle f, \phi_\mu^* \rangle_{\mathcal{H}} = \|\phi_\mu^*\|_{\mathcal{H}}.$$

■

B.6 Proof of Theorem A.7

Proof. Note $T_\varepsilon = T, \mu_{[T]}$ the density of $T_\# \mu$ w.r.t. λ . First, when ε is sufficiently small, T is close to the identity and is guaranteed to be a one-to-one. Using change of variable, we know that $T_\#^{-1} \pi$ admits a density $\pi_{[T^{-1}]}$ w.r.t. λ and

$$\pi_{[T^{-1}]}(x) = \pi(T(x)) \cdot |\det \nabla_x T(x)|, \forall x \in \Omega.$$

Remark B.3. It is easy to see that, if T is a one-to-one map, then

$$\forall x \in \Omega, (\mu_{[T]} \circ T)(x) = \mu(x).$$

Let's show that $\text{KL}(T_{\#}\mu||\pi) = \text{KL}(\mu||T_{\#}^{-1}\pi)$.

$$\begin{aligned}
\text{KL}(T_{\#}\mu||\pi) &= \int_{\Omega} \log \left(\frac{\mu_{[T]}(x)}{\pi(x)} \right) dT_{\#}\mu(x) \\
&= \int_{T^{-1}(\Omega)} \log \left(\frac{(\mu_{[T]} \circ T)(x)}{(\pi \circ T)(x)} \right) d\mu(x) \\
&= \int_{T^{-1}(\Omega)} \log \left(\frac{(\mu_{[T]} \circ T)(x)}{(\pi_{[T^{-1}]} \circ T^{-1} \circ T)(x)} \right) d\mu(x) \\
&= \int_{T^{-1}(\Omega)} \mu(x) \log \left(\frac{\mu(x)}{\pi_{[T^{-1}]}(x)} \right) dx \\
&= \int_{\Omega} \mu(x) \log \left(\frac{\mu(x)}{\pi_{[T^{-1}]}(x)} \right) dx \quad (T^{-1}(\Omega) = \{x \mid T^{-1}(x) \in \Omega\} = \Omega) \\
&= \text{KL}(\mu||T_{\#}^{-1}\pi).
\end{aligned}$$

For more details, see Lean proof⁶. Thus, we have

$$\begin{aligned}
\nabla_{\varepsilon} \text{KL}(\mu||T_{\#}^{-1}\pi) &= \nabla_{\varepsilon} \int_{\Omega} \mu(x) \log \left(\frac{\mu(x)}{\pi_{[T^{-1}]}(x)} \right) dx \\
&= \int_{\Omega} \mu(x) \nabla_{\varepsilon} [\log(\mu(x)) - \log(\pi_{[T^{-1}]}(x))] dx \\
&= - \int_{\Omega} \mu(x) \nabla_{\varepsilon} \log(\pi_{[T^{-1}]}(x)) dx \\
&= -\mathbb{E}_{x \sim \mu} [\nabla_{\varepsilon} \log(\pi_{[T^{-1}]}(x))] .
\end{aligned}$$

Now, let's compute $\nabla_{\varepsilon} \log(\pi_{[T^{-1}]}(x))$.

$$\begin{aligned}
\nabla_{\varepsilon} \log(\pi_{[T^{-1}]}(x)) &= \nabla_{\varepsilon} \log(\pi(T(x)) \cdot |\det(\nabla_x T(x))|) \\
&= \nabla_{\varepsilon} \log \pi(T(x)) + \nabla_{\varepsilon} \log |\det(\nabla_x T(x))| \\
&= \nabla_{T(x)} \log \pi(T(x))^{\top} \nabla_{\varepsilon} T(x) + \nabla_{\varepsilon} \log |\det(\nabla_x T(x))| \\
&= \nabla_{T(x)} \log \pi(T(x))^{\top} \nabla_{\varepsilon} T(x) + \frac{1}{\det(\nabla_x T(x))} \nabla_{\varepsilon} \det(\nabla_x T(x)) \\
&= \nabla_{T(x)} \log \pi(T(x))^{\top} \nabla_{\varepsilon} T(x) + \frac{1}{\det(\nabla_x T(x))} \sum_{ij} (\nabla_{\varepsilon} \nabla_x T(x)_{ij} C_{ij}) \\
&= \nabla_{T(x)} \log \pi(T(x))^{\top} \nabla_{\varepsilon} T(x) + \sum_{ij} \left(\nabla_{\varepsilon} \nabla_x T(x)_{ij} (\nabla_x T(x))_{ji}^{-1} \right) \\
&= \nabla_{T(x)} \log \pi(T(x))^{\top} \nabla_{\varepsilon} T(x) + \text{trace}((\nabla_x T(x))^{-1} \cdot \nabla_{\varepsilon} \nabla_x T(x)) ,
\end{aligned}$$

where C is the cofactor matrix of $\nabla_x T(x)$. Finally, the result of the theorem is a special case of the above result. Indeed, $\forall \phi \in \mathcal{H}$, if $T = I_d + \varepsilon \phi$, then

- $T(x)|_{\varepsilon=0} = x$;
- $\nabla_{\varepsilon} T(x) = \phi(x)$;
- $\nabla_x T(x)|_{\varepsilon=0} = I_d$;
- $\nabla_{\varepsilon} \nabla_x T(x) = \nabla_x \phi(x)$.

This gives

$$\nabla_{\varepsilon} \text{KL}(T_{\#}\mu||\pi)|_{\varepsilon=0} = -\mathbb{E}_{x \sim \mu} [\nabla \log \pi(x)^{\top} \phi(x) + \nabla \cdot \phi(x)] .$$

Applying Theorem A.6 ends the proof. ■

⁶gaetan-serre.fr/assets/Lean/SBS/html/KL.lean.html

B.7 Proof of Theorem 2.2

Proof. First, as Ω is a subset of a metric space (Euclidean space) and is compact, it is also complete for the induced metric. In addition, as it is connected, it is also path-connected. These properties combined with the fact that Ω is smooth ensure that Ω is a smooth complete manifold. Finally, as $(T_t)_{0 \leq t}$ is a locally Lipschitz family of diffeomorphisms representing the trajectories associated with the vector field ϕ_t , and as $\mu_t = T_{t\#}\mu$, then, a direct application of Theorem 5.34 from [36] gives that μ_t is the unique solution of the nonlinear transport equation

$$\begin{cases} \frac{\partial \mu_t}{\partial t} + \nabla \cdot (\mu_t \phi_t) &= 0, \forall t > 0, \\ \mu_0 &= \mu \end{cases},$$

where the divergence operator $(\nabla \cdot)$ is defined by duality against smooth compactly supported functions, i.e.

$$\forall \mu \in \mathcal{M}(\Omega), \forall \phi : \Omega \rightarrow \Omega, \forall \varphi \in C_c^\infty(\Omega), \langle T_{\nabla \cdot (\phi \mu)}, \varphi \rangle = -\langle T_\mu, \phi \cdot \nabla \varphi \rangle,$$

where $\mathcal{M}(\Omega)$ is the set of measures on Ω , for any μ in $\mathcal{M}(\Omega)$, T_μ is the distribution associated with μ , and, for any φ in $C_c^\infty(\Omega)$, $\langle T_\mu, \varphi \rangle = \int_\Omega \varphi \, d\mu$ (see also [37]). Furthermore, as $\mu_{i+1} = (I_d + \varepsilon \phi_{\mu_i}^*)_{\#} \mu_i$ (see Eq. 7), one can write

$$\begin{aligned} \int_\Omega \varphi \, d\mu_{i+1} &= \int_\Omega \varphi \circ (I_d + \varepsilon \phi_{\mu_i}^*) \, d\mu_i, \forall \varphi \in C_c^\infty(\Omega). \\ &\stackrel{\varepsilon \rightarrow 0}{\sim} \int_\Omega \varphi + \varepsilon (\nabla \varphi \cdot \phi_{\mu_i}^*) \, d\mu_i \quad (\text{Taylor expansion of } \varphi(x) \text{ at } x + \varepsilon \phi_{\mu_i}^*(x)) \\ &= \int_\Omega \varphi \, d\mu_i + \int_\Omega \varepsilon (\nabla \varphi \cdot \phi_{\mu_i}^*) \, d\mu_i \\ &= \int_\Omega \varphi \, d\mu_i - \int_\Omega \varepsilon \varphi \, d(\nabla \cdot (\mu_i \phi_{\mu_i}^*)) \\ \iff \int_\Omega \varphi \, d\mu_{i+1} - \int_\Omega \varphi \, d\mu_i &= -\varepsilon \int_\Omega \varphi \, d(\nabla \cdot (\mu_i \phi_{\mu_i}^*)). \end{aligned}$$

This shows that iteratively updates μ in the direction $I_d + \varepsilon \phi_{\mu_i}^*$, given a small ε , corresponds to a finite difference approximation of the nonlinear transport equation. \blacksquare

B.8 Proof of Theorem 2.3

Proof. Using the Leibniz integral rule, the time derivative of the KL-divergence writes

$$\begin{aligned} \frac{\partial \text{KL}(\mu_t || \pi)}{\partial t} &= \frac{\partial}{\partial t} \int_\Omega \log \frac{d\mu_t}{d\pi} \, d\mu_t \\ &= \int_\Omega \frac{\partial \mu_t(x)}{\partial t} \log \frac{\mu_t(x)}{\pi(x)} \, dx + \int_\Omega \mu_t(x) \frac{\partial \log \frac{\mu_t(x)}{\pi(x)}}{\partial t} \, dx \\ &= \int_\Omega \frac{\partial \mu_t(x)}{\partial t} \log \frac{\mu_t(x)}{\pi(x)} \, dx + \int_\Omega \mu_t(x) \frac{\partial \log \mu_t(x)}{\partial t} \, dx \\ &= \int_\Omega \frac{\partial \mu_t(x)}{\partial t} \log \frac{\mu_t(x)}{\pi(x)} \, dx + \int_\Omega \frac{\partial \mu_t(x)}{\partial t} \, dx \\ &= \int_\Omega \frac{\partial \mu_t(x)}{\partial t} \log \frac{\mu_t(x)}{\pi(x)} \, dx + \frac{\partial}{\partial t} \int_\Omega \mu_t \, dx \\ &= \int_\Omega \frac{\partial \mu_t(x)}{\partial t} \log \frac{\mu_t(x)}{\pi(x)} \, dx \quad \left(\text{as, } \forall t \geq 0, \int_\Omega d\mu_t = 1 \right). \end{aligned}$$

Furthermore, μ_t is the unique solution of the nonlinear transport equation of Theorem 2.2, where $\phi_{\mu_t}^* = S_{\mu_t} \nabla \log \frac{\pi}{\mu_t}$ (see Appendix B.5). Thus, we have

$$\begin{aligned}
\frac{\partial \text{KL}(\mu_t | \pi)}{\partial t} &= - \int_{\Omega} \nabla \cdot (\mu_t(x) \phi_{\mu_t}^*(x)) \log \frac{\mu_t(x)}{\pi(x)} dx \\
&= \int_{\Omega} \mu_t(x) \phi_{\mu_t}^*(x) \cdot \nabla \log \frac{\mu_t(x)}{\pi(x)} dx \quad (\phi_{\mu_t}^* \in \mathcal{S}_{\mu_t}) \\
&= \int_{\Omega} \phi_{\mu_t}^*(x) \cdot \nabla \log \frac{\mu_t(x)}{\pi(x)} d\mu_t(x) \\
&= \left\langle \iota \phi_{\mu_t}^*, \nabla \log \frac{\mu_t}{\pi} \right\rangle_{L_{\mu_t}^2(\Omega, \Omega)} \\
&= \left\langle \phi_{\mu_t}^*, S_{\mu_t} \nabla \log \frac{\mu_t}{\pi} \right\rangle_{\mathcal{H}} \\
&= \left\langle \phi_{\mu_t}^*, -S_{\mu_t} \nabla \log \frac{\pi}{\mu_t} \right\rangle_{\mathcal{H}} \\
&= - \left\langle \phi_{\mu_t}^*, \phi_{\mu_t}^* \right\rangle_{\mathcal{H}} \\
&= - \|\phi_{\mu_t}^*\|_{\mathcal{H}}^2 \\
&= -\mathfrak{K}(\mu_t | \pi).
\end{aligned}$$

■

B.9 Proof of Lemma 2.4

Proof. We recall that, using Appendix B.5,

$$\mathfrak{K}(\mu | \pi) = \|\phi_{\mu}^*\|_{\mathcal{H}}^2 = \mathbb{E}_{x \sim \mu} [\mathcal{A}_{\pi} \phi_{\mu}^*].$$

The right implication is straightforward. Assume that $\mu = \pi$. We know that ϕ_{μ}^* is in $\mathcal{S}(\mu) = \mathcal{S}(\pi)$, thus, using Lemma A.3, we have that

$$\mathbb{E}_{x \sim \mu} [\mathcal{A}_{\pi} \phi_{\mu}^*] = \mathfrak{K}(\mu | \pi) = \mathbb{E}_{x \sim \pi} [\mathcal{A}_{\pi} \phi_{\mu}^*] = 0.$$

The left implication is more involved. Assume that $\mathfrak{K}(\mu | \pi) = 0$. In Appendix B.5, we have shown that

$$\phi_{\mu}^* = S_{\mu} \nabla \log \frac{\pi}{\mu}.$$

This implies that

$$\mathfrak{K}(\mu | \pi) = \|\phi_{\mu}^*\|_{\mathcal{H}}^2 = \left\langle S_{\mu} \nabla \log \frac{\pi}{\mu}, S_{\mu} \nabla \log \frac{\pi}{\mu} \right\rangle_{\mathcal{H}} = \left\langle \nabla \log \frac{\pi}{\mu}, \iota S_{\mu} \nabla \log \frac{\pi}{\mu} \right\rangle_{L_{\mu}^2(\Omega, \Omega)}.$$

Thus, one can rewrite the KSD as

$$\mathfrak{K}(\mu | \pi) = \int_{\Omega} \int_{\Omega} \nabla \log \frac{\pi}{\mu}(x)^{\top} k(x', x) \nabla \log \frac{\pi}{\mu}(x') d\mu(x) d\mu(x').$$

Since k is positive definite, we have that

$$\mathfrak{K}(\mu | \pi) = 0 \iff \nabla \log \frac{\pi}{\mu}(x) = 0, \forall x \in \Omega.$$

Moreover, as the density of μ is supported over Ω , there is no set $E \subset \Omega$ such that $\lambda(E) > 0$ and $\mu(E) = 0$. Thus, a predicate $P(x)$ is true for almost all $x \in \Omega$, w.r.t. μ if and only if $P(x)$ is true for almost all x in Ω , w.r.t. λ .

Finally, if $\forall x \in \Omega, \nabla \log \frac{\pi}{\mu}(x) = 0$, it implies that $\exists c \in \mathbb{R}_{>0}$ such that, $\mu(x) = c\pi(x)$. As $\mu(\cdot)$ and $\pi(\cdot)$ are probability densities over Ω , $c = 1$:

$$\mu(\Omega) = 1 = \int_{\Omega} \mu(x) dx = c \int_{\Omega} \pi(x) dx = c.$$

Thus,

$$\nabla \log \frac{\pi}{\mu}(x) = 0 \iff \pi(x) = \mu(x), \bar{\nabla}x \in \Omega.$$

For more details, see Lean proof⁷. ■

B.10 Proof of Lemma 2.5

Proof. We first show that π is a fixed point of $(\mu : \mathcal{P}_2(\Omega)) \mapsto \Phi_t(\mu)$, i.e. $\Phi_t(\pi) = \pi$. To do so, recall that

$$\mathfrak{K}(\pi|\pi) = \|\phi_\pi^*\|_{\mathcal{H}}^2.$$

Using the right implication of Lemma 2.4, we have that

$$\|\phi_\pi^*\|_{\mathcal{H}}^2 = 0,$$

which implies that

$$\iff \phi_\pi^*(x) = 0, \bar{\nabla}_\pi x \in \Omega.$$

Thus, $\bar{\nabla}_\pi x \in \Omega$,

$$T_\pi(x) = x + \varepsilon \phi_\pi^*(x) = x,$$

implying $\Phi_t(\pi) = \pi$.

Then, suppose that $\exists \nu \in \mathcal{P}_2(\Omega)$ such that $\nu \neq \pi$ and $\Phi_t(\nu) = \nu$ for any $t \geq 0$. We have that

$$\frac{\partial \text{KL}(\Phi_t(\nu)||\pi)}{\partial t} = 0 = -\mathfrak{K}(\nu||\pi).$$

However, using the left implication of Lemma 2.4, we obtain a contradiction.

For more details, see Lean proof⁷. ■

B.11 Proof of Theorem 2.6

Proof. By construction of $\mathcal{P}_2(\Omega)$, $\text{KL}(\mu||\pi)$ is finite. Moreover, as stated in Theorem 2.3, $t \mapsto \text{KL}(\mu_t||\pi)$ is decreasing. Thus, it exists a positive real constant c , such that, for any sequence $(t_n)_{n \in \mathbb{N}}$ such that $t_n \rightarrow \infty$, $\text{KL}(\mu_{t_n}||\pi) \rightarrow c$. It implies that, for any such sequence $(t_n)_{n \in \mathbb{N}}$, it exists a subsequence $(t_k)_{k \in \mathbb{N}}$ such that $\mu_{t_k} \rightarrow \mu_\infty$, meaning that $\Phi_t(\mu) \rightarrow \mu_\infty$ (see Theorem 2.6 [3]). Therefore, μ_∞ is a fixed point of Φ_t , for any $t \geq 0$ and any $\mu \in \mathcal{P}_2(\Omega)$ such that $\text{KL}(\mu||\pi)$ is finite. Finally, using Lemma 2.5, we have that $\mu_\infty = \pi$. ■

B.12 Proof of Theorem 2.7

Proof. In order to apply any SVGD theoretical results, we need to ensure that every assumptions are satisfied. First, we know by hypothesis that $\mu_0 \in H^1(\Omega)$ and the fact that $f \in C^0(\Omega) \cap W^{1,4}(\Omega)$ ensure that $\pi \in H^1(\Omega)$ as well (see Appendix B.2). We assume the kernel k to satisfy the conditions of Appendix A.2.3. We know by hypothesis and by construction of the BD that $\text{supp}(\mu_0) = \text{supp}(\pi) = \Omega$. Finally, $\text{KL}(\mu_0||\pi)$ is finite. This allows to use Theorem 2.2 and Theorem 2.6, or any other theoretical results relative to SVGD.

Using the strong law of large numbers, one can show that, for any $i \in \mathbb{N}$, the discrete measure $\hat{\mu}_i$ converges almost surely to μ_i as $\hat{\mu}_i$ is the empirical measure arising from an i.i.d. sequence of samples from μ_i . Thus, $\hat{\mu}_i \xrightarrow[N \rightarrow \infty]{a.s.} \mu_i$. Moreover, in Appendix B.7, we showed that

$$\forall \varphi \in C_c^\infty(\Omega), \langle T_{\mu_{i+1}-\mu_i}, \varphi \rangle \xrightarrow[\varepsilon \rightarrow 0]{} \langle T_{\nabla \cdot (\mu_i \phi_{\mu_i}^*)}, \varphi \rangle.$$

Let ν be the net extension of $(\mu_i)_{i \in \mathbb{N}}$ as ε tends to 0:

$$\begin{aligned} \nu_\bullet : \mathbb{R}_{\geq 0} &\rightarrow \mathcal{P}_2(\Omega), \\ t &\mapsto \mu_{\lfloor t/\varepsilon \rfloor}. \end{aligned}$$

We have that

$$\{\mu_i | i \in \mathbb{N}\} = \{\nu_t | t \in \mathbb{R}_{\geq 0}\}.$$

⁷gaetan-serre.fr/assets/Lean/SBS/html/KSD.lean.html

Moreover, for any $t \in \mathbb{R}_{\geq 0}$ and any $\varphi \in C_c^\infty(\Omega)$,

$$\begin{aligned}
\lim_{\varepsilon \rightarrow 0} \langle T_{\nu_{t+\varepsilon} - \nu_t}, \varphi \rangle &= \lim_{\varepsilon \rightarrow 0} \langle T_{\mu_{\lfloor (t+\varepsilon)/\varepsilon \rfloor} - \mu_{\lfloor t/\varepsilon \rfloor}}, \varphi \rangle \\
&= \lim_{\varepsilon \rightarrow 0} \langle T_{\mu_{\lfloor t/\varepsilon \rfloor + 1} - \mu_{\lfloor t/\varepsilon \rfloor}}, \varphi \rangle \\
&= -\varepsilon \left\langle T_{\nabla \cdot (\mu_{\lfloor t/\varepsilon \rfloor} \phi_{\mu_{\lfloor t/\varepsilon \rfloor}}^*)}, \varphi \right\rangle \\
&= -\varepsilon \langle T_{\nabla \cdot (\nu_t \phi_{\nu_t}^*)}, \varphi \rangle.
\end{aligned}$$

This allows to state on the derivative of ν :

$$\begin{aligned}
\lim_{\varepsilon \rightarrow 0} \int_{\Omega} \varphi d \frac{\nu_{t+\varepsilon} - \nu_t}{\varepsilon} &= - \int_{\Omega} \varphi d \nabla \cdot (\nu_t \phi_{\nu_t}^*), \\
\implies \frac{\partial \nu_t}{\partial t} &\xrightarrow{\varepsilon \rightarrow 0} -\nabla \cdot (\nu_t \phi_{\nu_t}^*).
\end{aligned}$$

Thus, as $\nu_0 = \mu_0$, ν_\bullet tends to a solution of Eq. 3, when ε tends to 0. Finally, by construction of ν_\bullet and as $(\mu_t)_{t \in \mathbb{R}_{\geq 0}}$ is the unique solution of the nonlinear transport equation, we have that

$$(\mu_i)_{i \in \mathbb{N}} \xrightarrow{\varepsilon \rightarrow 0} (\mu_t)_{t \in \mathbb{R}_{\geq 0}}.$$

This result is expected as $(\mu_i)_{i \in \mathbb{N}}$ is a discretization of $(\mu_t)_{t \in \mathbb{R}_{\geq 0}}$ (see Appendix B.7).

Now, using Theorem 2.6, we have that $(\mu_i)_{i \in \mathbb{N}} \xrightarrow[\substack{\varepsilon \rightarrow 0 \\ i \rightarrow \infty}]{\pi} \pi$ and thus, $(\hat{\mu}_i)_{i \in \mathbb{N}} \xrightarrow[\substack{N \rightarrow \infty \\ \varepsilon \rightarrow 0 \\ i \rightarrow \infty}]{\pi} \pi$. The fact that the

Boltzmann distribution ensures that π tends to a distribution supported on X^* as κ tends to ∞ (see Properties A.1) gives the desired result.

■